AD-A133 339   MISSISSIPPI SOUND WAVE-HINDCAST STUDY: MAIN TEXT AND   1/1
               APPENDICES A AND B(U) ARMY ENGINEER WATERWAYS
               EXPERIMENT STATION VICKSBURG MS HYDRA.. R E JENSEN
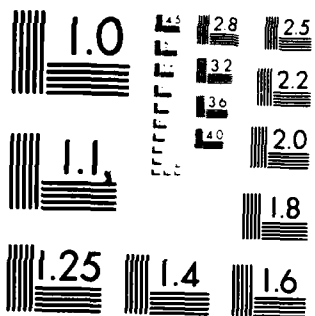UNCLASSIFIED   APR 83 WES/TR/HL-83-8-APP-A/B   F/G 8/10   NL

END
DATE
FILMED
10-83
DTIC

MICROCOPY RESOLUTION TEST CHART

NATIONAL BUREAU OF STANDARDS 1963 A

TECHNICAL REPORT HL-83-8

MISSISSIPPI SOUND
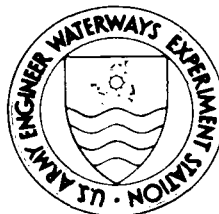# WAVE-HINDCAST STUDY

MAIN TEXT AND APPENDICES A AND B

by

Robert E. Jensen

Hydraulics Laboratory
U. S. Army Engineer Waterways Experiment Station
P. O. Box 631, Vicksburg, Miss. 39180

April 1983

Final Report

DTIC
ELECTE
OCT 1 1 1983
S   D

D

83 10   010

REPORT DOCUMENTATION PAGE		READ INSTRUCTIONS BEFORE COMPLETING FORM
1. REPORT NUMBER Technical Report HL-83-8	2. GOVT ACCESSION NO. AD·A133339	3. RECIPIENT'S CATALOG NUMBER
4. TITLE (and Subtitle) MISSISSIPPI SOUND WAVE-HINDCAST STUDY--MAIN TEXT AND APPENDICES A AND B		5. TYPE OF REPORT & PERIOD COVERED Final report
		6. PERFORMING ORG. REPORT NUMBER
7. AUTHOR(a) Robert E. Jensen		8. CONTRACT OR GRANT NUMBER(s)
9. PERFORMING ORGANIZATION NAME AND ADDRESS U. S. Army Engineer Waterways Experiment Station Hydraulics Laboratory P. O. Box 631, Vicksburg, Miss. 39180		10. PROGRAM ELEMENT, PROJECT, TASK AREA & WORK UNIT NUMBERS
11. CONTROLLING OFFICE NAME AND ADDRESS U. S. Army Engineer District, Mobile P. O. Box 2288 Mobile, Ala. 36628		12. REPORT DATE April 1983
		13. NUMBER OF PAGES 878
14. MONITORING AGENCY NAME & ADDRESS(If different from Controlling Office)		15. SECURITY CLASS. (of this report) Unclassified
		15a. DECLASSIFICATION/DOWNGRADING SCHEDULE

16. DISTRIBUTION STATEMENT (of this Report)

Approved for public release; distribution unlimited.

17. DISTRIBUTION STATEMENT (of the abstract entered in Block 20, if different from Report)

18. SUPPLEMENTARY NOTES
A limited number of copies of Appendices C-G were published under separate cover. Copies of this report and Appendices C-G are available from National Technical Information Service, 5285 Port Royal Road, Springfield, Va. 22161.

19. KEY WORDS (Continue on reverse side if necessary and identify by block number)

Mississippi Sound
Shallow Water Wave Model
Wave Hindcast Statistics

20. ABSTRACT (Continue on reverse side if necessary and identify by block number)

'Long-term overwater winds were generated using data from land-based meteorological stations adjacent to Mississippi Sound. A parametric shallow-water wave model was developed and verified employing extensive measured wave data. The shallow-water wave model and the simulated wind fields were utilized to calculate 20 years (1956-1975) of hindcast wave data for 23 sites in Mississippi Sound. Analyses of the hindcast wave data are presented.

PREFACE

In late 1980, a study to produce a wave climate for the Mississippi Sound region was initiated at the U. S. Army Engineer Waterways Experiment Station (WES). This study, the Mississippi Sound Wave-Hindcast Study, was authorized by the U. S. Army Engineer District, Mobile, as part of a larger study investigating the Mississippi Sound waters. The Mobile District authorized the funds throughout the study.

The report describes the methodology of the wind-field development and the shallow-water modeling technique and presents wave hindcast statistics for the period of 1956-1975. This work was done in the Hydraulics Laboratory under the direction of Mr. H. B. Simmons, Chief of the Hydraulics Laboratory, Dr. R. W. Whalin, former Chief of the Wave Dynamics Division, and Mr. C. E. Chatham, Acting Chief of the Wave Dynamics Division. This report was prepared by Dr. R. E. Jensen. Rebecca Brooks, W. D. Corson, D. S. Ragsdale, and H. Messing provided additional assistance in the preparation of this report.

Commanders and Directors of WES during the conduct of the study and the preparation and publication of this report were COL Nelson P. Conover, CE, and COL Tilford C. Creel, CE. Technical Director was Mr. F. R. Brown.

Accession For	
NTIS GRA&I	X
DTIC TAB	☐
Unannounced	☐
Justification	
By	
Distribution/	
Availability Codes	
Dist	Avail and/or Special
A	

1

CONTENTS

---

* A limited number of copies of Appendices C-G were published under separate cover. Copies are available from National Technical Information Service, 5285 Port Royal Road, Springfield, Va. 22151.

CONVERSION FACTORS, U. S. CUSTOMARY TO METRIC (SI)
UNITS OF MEASUREMENT

U. S. customary units of measurement used in this report can be converted to metric (SI) units as follows:

Multiply	By	To Obtain
feet	0.3048	metres
knots (international)	0.514444	metres per second
miles (U. S. nautical)	1.852	kilometres
miles (U. S. statute)	1.609344	kilometres
miles per hour	1.609344	kilometres per hour
miles per hour	0.8689	knots per hour
square feet per second	0.09290304	square metres per second
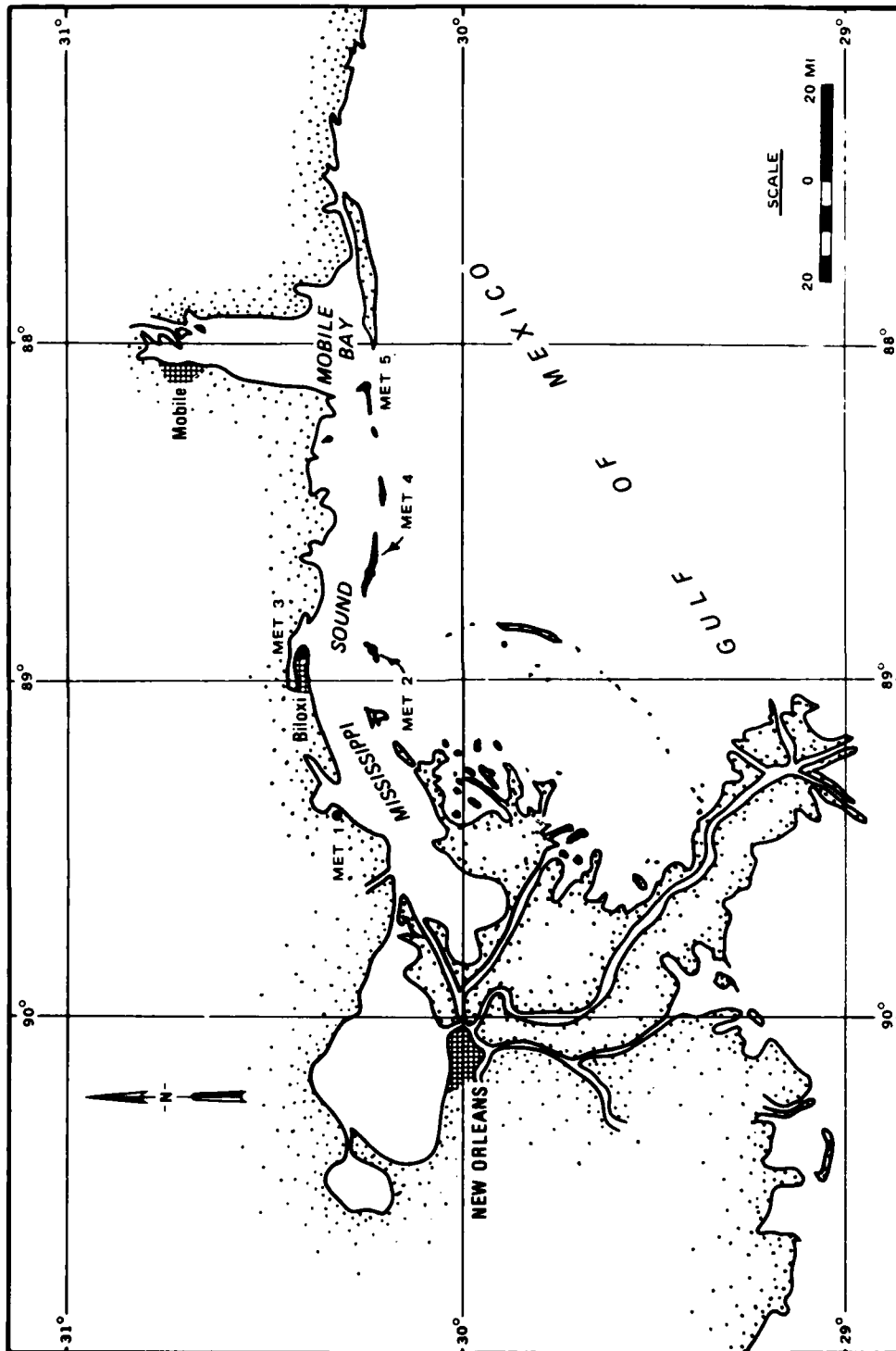
Figure 1. Location of wind and surf zone wave data

4

MISSISSIPPI SOUND WAVE-HINDCAST STUDY

PART I: INTRODUCTION

1. The primary purpose of this study is to provide a 20-year wave climate in the Mississippi Sound region (Figure 1). Secondary efforts include the development of a representative wind field over the study area and the development of a wave modeling technique that provides an accurate representation of the mechanisms involved in shallow-water wave growth and transformations.

2. The sparseness of wave information in Mississippi Sound becomes critical to the design of coastal or offshore structures and also to the operation of dredging and shipping activities. A search for available wave information in the Sound was performed, where, over a 20-year duration, only 27 recorded visual ship observations reflected wave conditions. Wave gaging was performed with limited success in 1980 by the Raytheon Corporation (U. S. Army Engineer District, Mobile, 1981) as part of data collection effort to calibrate and verify a numerical model.

3. To accurately describe the wave climate within Mississippi Sound, two types of techniques can be employed--wave gaging and wave hindcasting. Although a network of wave gages might eventually provide a good data source, the expense involved would make it economically prohibitive to provide detailed coverage of the entire Mississippi Sound region. Even if such a wave gage network were established, there would be a lag time of many years before sufficient wave information was available for design purposes.

4. A viable alternative to wave-gaging Mississippi Sound would be to hindcast the wave climate. Many different techniques are presently available to generate wave characteristics. These techniques can be subdivided into three categories: empirical, parametric, and numerical. All three types of wave-hindcasting methods have certain advantages and disadvantages associated with their operation. A discussion of these

5

techniques will be presented later in this report. A parametric shallow-water wave model was developed to perform the 20-year hindcast for the Mississippi Sound region to minimize computational costs without loss in describing the physics of the problem.

5. The use of hindcast techniques to estimate wave heights assumes that the coupling between the atmospheric boundary layer and waves generated by the motion of this boundary is known. Other factors, such as dispersion effects (finite water depths), bottom effects (friction), and interactions between different spectral wave components must also be considered. If all the linear and nonlinear wave transformation mechanisms are adequately described and if the atmospheric motion over the Sound is known, then a reliable estimate of wave conditions can be made. In any estimate of wave characteristics (height, period, and direction of wave propagation) there will always be some degree of error. Because of the paucity and questionable reliability of measured wave data within the Sound (paragraphs 47-51), an extensive error analysis cannot be made. All assumptions and mechanisms governing the hindcast technique have been analyzed in the "Wave Data Acquisition and Hindcast for Saginaw Bay Study" (Garcia and Jensen, in preparation). Because of the problems associated with the measured data within Mississippi Sound, the error analysis performed in the Saginaw Bay study is presented to ensure that the modeling technique adequately describes the processes involved in finite water depth wave generation.

6. PART II of this report deals with the wind information analysis, PART III discusses the shallow-water wave modeling technique, PART IV discusses the 20-year wave hindcast products, and PART V discusses results.

PART II: ESTIMATION OF WINDS

7. The recovery and subsequent analysis of wind data become an integral part in the Mississippi Sound Wave-Hindcast Study. The lack of continuous long-term wind observations over the region forces the conclusion that winds over Mississippi Sound must be estimated from alternate sources of data. Two sources of data with a sufficient length of record (20 years) are synoptic weather maps and wind observations at adjacent land stations. The conversion of a synoptic weather map from its initial state to a finalized wind field would require extensive hand digitization accompanied by an inordinate amount of computational time. Therefore, the only feasible sources of data for the estimation of winds over Mississippi Sound are from land-situated wind observations from data sources around the study region.

8. Three long-term meteorological sites were selected: Keesler Air Force Base (KAFB), Biloxi, Mississippi; Mobile, Alabama; and New Orleans, Louisiana (Figure 1). The primary source of the wind information was taken from the Biloxi stations. The Biloxi station is geographically the closest meteorological station to the study area. The weather conditions over the Sound would be better represented employing this data set over the wind data obtained from either Mobile, Alabama, or New Orleans, Louisiana. Since gaps in the wind record occurred, it was necessary to supplement the KAFB, Biloxi, data with either the Mobile or New Orleans wind information. The data supplementing procedure implies that winds in the area are nearly uniform both in intensity and direction. This assumption is verified in Table 1 where wind conditions (speed and direction) were randomly selected (24 hr of data per set per year). If the KAFB, Biloxi, wind data are assumed to be the norm, the data reveal that average wind speed differences of 12 percent and 4 percent are found at Mobile and New Orleans, respectively. The mean wind direction differences are approximately 3 to 4 deg while the standard deviation around the mean is 36 to 44 deg. The large variation in the standard deviation spans approximately two wind angle classes (winds are given in 16 direction bands at 22.5-deg increments) and are primarily

7

Table 1

Differences in Wind Speed and Direction†

Location	Wind Speed Difference†† percent	Wind Direction Difference	
		Mean deg	Standard Deviation deg
New Orleans	+4	-4	±44
Mobile	+12	-3	±36

† Differences between cited location and Biloxi.
†† All wind speeds adjusted to 33 ft.

caused by low wind speed conditions wherein the wind direction becomes
highly variable and is difficult to determine.

9.   During the period 1956-1965, wind data are recorded every
hour. The wind data over this time interval are averaged over a 3-hr
interval (using the wind data from the three preceding hourly records).
The wind data from 1965-1975 are given in 3-hr intervals; thus the aver-
aging step was not performed. A 20-year record of wind speed and direc-
tion recorded every 3 hr is generated and stored on magnetic tape for
further analysis.

10.   Wind speed and direction changes in the data are primarily
caused by the slow migration of weather patterns. The passage of frontal
weather patterns, sea breezes, and other small-scale meteorological con-
ditions are included in the wind data although their overall influence
of larger scale meteorological conditions would be diminished. Also,
tropical storm conditions cannot be classified within this constraint.
During the 20-year hindcast study (1956-1975), numerous tropical storms
passed through or passed in close proximity to the Mississippi Sound
region. It was decided* that the winds would be treated as if they were
generated from extratropical storm conditions. These data are shown in
Table 2 (Neumann et al. 1978).

11.   Once the 20-year wind data are assembled, adjustments must be

---

* R. Champion. 1982. Personal communication, U. S. Army Engineer Dis-
   trict, Mobile, CE, Mobile, Alabama.

8

Table 2

Tropical Storm Condition Data

Year	Month	Day	New Orleans		Biloxi		Mobile	
			Max Wind knots	Date day/hour	Max Wind knots	Date day/hour	Max Wind knots	Date day/hour
1956	06	13-14	19	13/14	23	13/15	22	13/14
1956	09	23-25	42	24/2	31	24/9	35	24/14
1957	09	7-8	28	8/0	12	7/16	17	8/9
1957	09	16-19	22	18/3	29	18/10	30	18/10
1959	05	30-31	24	31/5	19	31/10	20	31/8-15
1959	10	6-8	14	6/12	14	6/12	18	7/16
1960	09	14-15	15	15/4-11	36	15/14	30	15/9
1960	09	25-26	14	25/19	14	25/19	20	25/18
1964	09	10-12	14	12/15	13	12/9	20	12/4
1964	10	3-5	35	4/2	33	4/17	35	4/19
1964	11	5-6	17	5/3-5	5	--	23	5/12-15
1965	06	14-16	11	15/15	13	14/13	15	14/15
1965	09	8-12	60	10/0	30	9/23-10/1	28	10/0
1965	09	28-29	17	29/0	23	29/14	18	29/18
1969	08	16-18	30	17/21	70	17/23	34	18/0
1969	09	5-6	13	5/15	14	5/15	10	6/9-12
1969	10-11	30-1	15	30/21-1/3	14	1/4	15	1/3-6
1970	07	21-22	8	--	10	21/13	12	21/12
1971	09	4-6	14	6/12	*	*	13	5/12
1971	09	16-17	25	16/9-12	*	*	24	16/18
1972	06	18-20	17	19/15	*	*	16	19/9-18
1974	09	7-8	27	7/21	15	7/15-18	19	7/12
1975	09	22-24	23	22/18	30	23/2	21	23/0

* Data not available.

9

made, such as transforming wind speeds from the given elevation to the standardized 10-m elevation, converting from overland to overwater wind speeds, adjusting for air-sea temperature differences, and nonconstant drag coefficients. The procedure for converting given wind speeds to "wave-model-ready" winds follows that described in Resio and Vincent (1976) and U. S. Army Coastal Engineering Research Center (CERC), CETN-I-5 (1981).

12. No long-term sea temperature data were available to compute stable, neutral, or unstable air-sea temperature conditions. It was assumed that during the 20-year hindcast, air-sea conditions were unstable (as described in U. S. Army CERC CETN-I-5), thus an increase of 10 percent was added to the resulting wind speed.

13. It also must be noted that only wind conditions coming from the west, clockwise to the east (270 deg $\leq \theta_w \leq$ 90 deg, where θ_w is the predominant wind direction), were converted from overland to overwater winds. All other wind conditions come from overwater areas relative to KAFB, Biloxi, as shown in Figure 1, and are not adjusted.

14. In summary, the 20-year wind conditions are derived from a single source (Biloxi, Mississippi, KAFB), and supplemented with two additional land stations (Mobile and New Orleans). The winds over the study area were shown to be uniform in speed and direction (Table 1). Wind conditions are then converted from overland to overwater winds and adjusted for a nonconstant drag coefficient and unstable air-sea temperature differences. From this analysis a continuous 20-year record is obtained of surface winds derived from all available measured wind information in the Mississippi Sound region.

PART III: SHALLOW-WATER WAVE MODELING TECHNIQUE

Introduction

15. The predictions of shallow-water wave characteristics have
become a focal point of research activities across the world. Because
construction, shipping, and dredging operation costs have drastically
increased over the years, coastal engineers have been faced with more
accurately defining the shallow-water wave climate. A better under-
standing of shallow-water wave growth and transformation mechanisms is
slowly evolving through controlled wave-measuring programs such as the
Atlantic Remote Sensing Land-Ocean Experiment (Vincent and Lichy 1981).
However, not all of the questions have been answered, and it will take
some time before all shallow-water wave transformation mechanisms are
quantified. In light of this, the shallow-water wave modeling technique
(SWWM) employed in this study adopts "state-of-the-art" mechanisms cur-
rently available. The main intent in the development of the SWWM is to
describe the physical processes as accurately as possible while simpli-
fying the computational procedures to a degree where a long-term hindcast
study is economically feasible.

16. This part of the report is subdivided into three sections:
(a) the discussion of the theoretical aspects of the SWWM, (b) the model
setup applied specifically to Mississippi Sound, and (c) calibration and
verification to existing measured and observed wave conditions.

17. The existing shallow-water* wave prediction techniques can be
classified into three categories--empirical, numerical, and parametric.
A brief review is given below, but a more detailed description of these
techniques can be found in Hsiao (1978) and Vincent (1982).

18. The most widely used technique to generate shallow-water wave
conditions is the empirical method first described by Bretschneider
(1954). Since that time, this approach has been revised (CERC 1977,

---

* Shallow water is defined as water depth conditions where dispersion
  effects become important (or changes in the phase and group wave
  celerities become dependent on changes in the water depth).

11

CERC CETN-I-6 1981). The significant wave height (H_s)* and significant
wave period (T_s) are estimated by empirical relationships between wave
height and wind speed, duration, and fetch. Also included in this
modeling technique is the influence of bottom friction mechanisms on
wave dissipation formulated by Bretschneider and Reid (1954).

19. The Bretschneider empirical shallow-water wave method is
based only on experimental data and no consideration of the physical
processes involved in wave development, such as generation and interac-
tions, is included in the technique.

20. Collins (1972) developed a finite depth wave model by
numerically solving the energy balance equation. The model included the
effect of wind generation similar to that employed by Barnett (1968).
Also, the transformation mechanisms modeled included wave refraction,
shoaling, bottom friction, and wave breaking. Another shallow-water
wave model based on the ray technique was developed by Cavalri and
Rizzoli (1981). Their model included the same processes as Collins'
version. One process that was not considered in either model was the
incorporation of the nonlinear energy transfers, or wave-wave interac-
tions (Hasselmann 1962). The influence of this mechanism has been shown
to be amplified in a finite water depth wave environment (Heterich and
Hasselmann 1980).

21. A parametric wave prediction model was first developed by
Hasselmann et al. (1976) for deepwater wave conditions. More recently
Hsiao (1978) and Shemdin et al. (1980) have adopted the original work
of Hasselmann et al. (1976) to finite water depths. The effect due to
wind generation, refraction, shoaling, nonlinear bottom interactions
(friction, percolation, viscoelasticity, and scattering), and nonlinear
wave-wave interactions (Heterich and Hasselmann 1980) were formulated in
the model. The inhomogeneous wave equation was solved numerically in
one dimension using a Runge-Kutta (numerical approximation method) type
of approach of successive approximations.

---

* For convenience, symbols and unusual abbreviations are listed and de-
  fined in the Notation (Appendix B).

22. No direct measurements can be made to verify the relative importance of each transformation mechanism; thus calibration and verification of this complex parametric model can be very difficult. One has to consider parameters at each selected site (such as bottom topography and sediment size and type) and continually make adjustments to the model for changes in time at that site. Therefore this technique is restricted to the computation of site-specific modeling and is difficult to employ for large geographical areas unless extensive measured data exist.

23. Since the above approaches to an accurate physical estimation of wave conditions in a large geographical area are inappropriate, an alternate approach to the problem of long-term wave hindcasting was developed specifically to meet the needs of the Mississippi Sound Wave-Hindcast Study. It should be recognized at the outset of this discussion that in order to maximize computational efficiency, a new approach to shallow-water wave modeling was developed. The key to this new approach is that the resulting wave conditions are produced by transformation mechanisms rather than transforming wave conditions during wave propagation. Computationally, it is more efficient to transform wave conditions from one location to another than it is to simultaneously propagate and transform sets of wave conditions from a given location to the next. Thus a shallow-water wave modeling technique was developed that includes wave growth, nonlinear transfers of energy, shoaling, refraction, energy dissipation resulting from wave decay (if during growth the spectrum is fully saturated), bottom friction, and wave breaking. Most transformation mechanisms are evaluated parametrically, while the remaining mechanisms are determined from empirically derived relationships.

24. Prior to the discussion of the transformation mechanisms, it is necessary to discuss the assumptions governing the SWWM results. Wind conditions are assumed to be uniform over Mississippi Sound. These conditions are typical of those generated from slowly moving extratropical storm systems. The winds also are assumed to remain constant for each 3-hr observation. Wave propagation is assumed to be restricted to the

13

direction described by the winds. Over each given fetch length (dependent on a wind angle class), the bottom topography is represented by straight and parallel bottom contours. Mississippi Sound is assumed to be a closed system, whereby all wave conditions found in the Sound are generated within its boundaries. No energy is permitted to propagate through the barrier island system to the south or from the east, due to Mobile Bay (Figure 1). Without a comprehensive wave gaging study in and around the Mississippi Sound region, an accurate assessment of this assumption cannot be made. The intent of the given assumptions is not to overly simplify the generation of a long-term hindcast for Mississippi Sound, but make it economically feasible without restricting the overall physics of the problem.

Theory

25. This section describes the theory employed in the SWWM. There are five basic parts to the SWWM: (a) wave growth, (b) application of conservative and nonconservative mechanisms on the growing energy, (c) construction of a one-dimensional energy density spectrum based on available energy, (d) application of an additional atmospheric source term on the spectrum, and (e) limitation of the energy due to wave breaking.

26. Hasselmann et al. (1976) introduced a parametric model of wind-wave generation, relating the rate of energy growth to nondimensional characteristics of the wind field. This energy growth (in space or time) is governed by a self-similar process and verified through extensive prototype data (Hasselmann et al. 1973 and 1976). In these studies, the dominant energy input on the forward face of the spectrum is related to convergence of energy flux due to nonlinear, resonant wave-wave interactions (Figure 2) of the form described by Hasselmann (1962). Work conducted by Mitsuyasu (1968, 1969) and Kitaigordskii (1962) also displayed similar results. Although these formulations are governed for deepwater wave conditions, they are used in the SWWM simply because the only formulation of the nonlinear transfers in shallow water are based

14

| | I
ENERGY GAINED ON FORWARD FACE OF SPECTRUM DUE TO WAVE-WAVE INTER-ACTION SOURCE | II
DYNAMIC EQUILIBRIUM MAINTAINED BETWEEN ATMOSPHERIC INPUT AND WAVE-WAVE INTERACTION SINK | III
ENERGY INPUT FROM WAVE-WAVE INTER-ACTIONS LOST TO VISCOUS AND TURBU-LENT DISSIPATION |
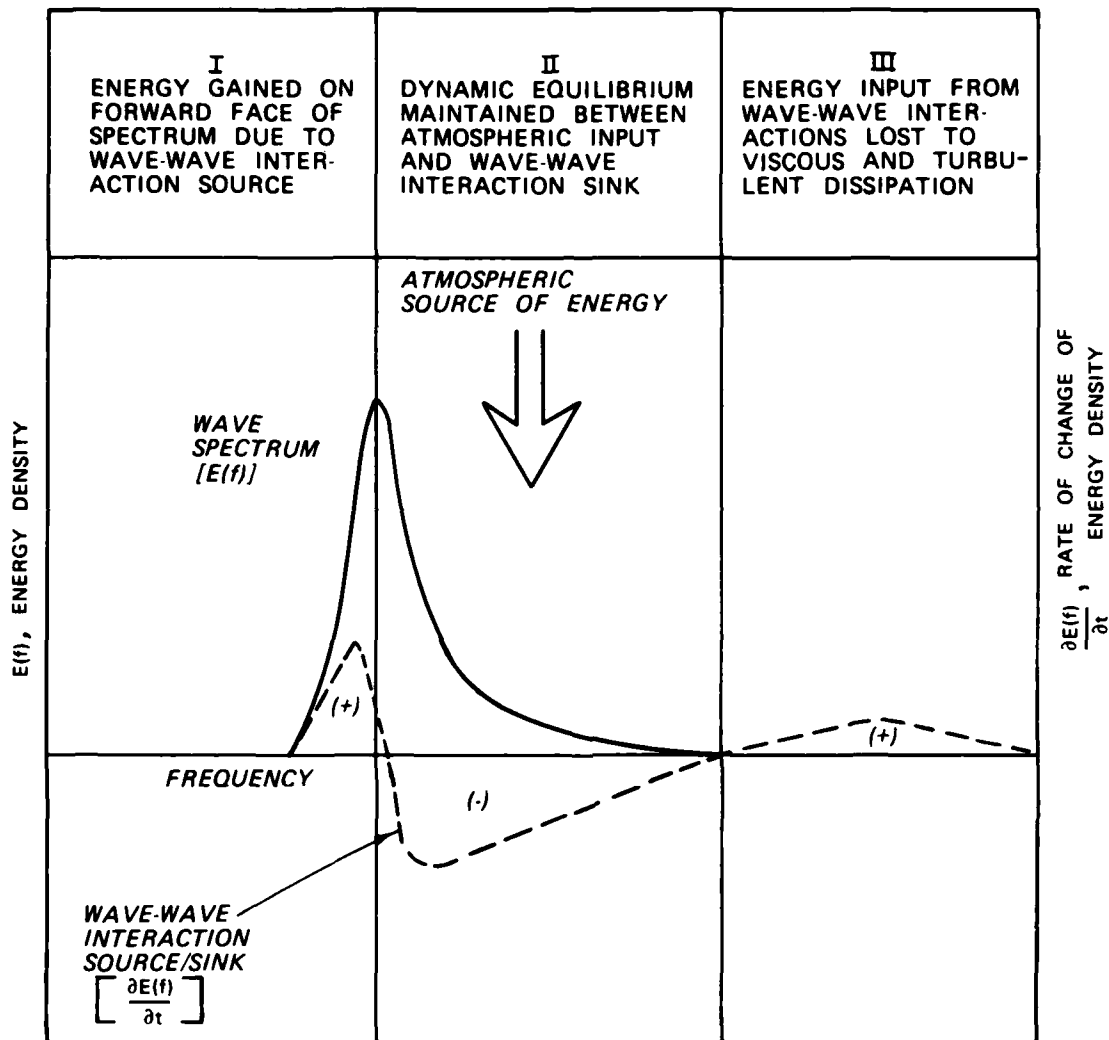
Figure 2.   Schematic representation of the nonlinear
wave-wave interaction

specifically on JONSWAP-type wave spectra. The parameterizations of the
shallow-water nonlinear transfers become too complex and require addi-
tional computational time to resolve. Also, the JONSWAP-type spectra
contain three free parameters which are based primarily on open-ocean,
deepwater spectra wave conditions that are not appropriate to Mississippi
Sound.

27.   The rate of wave growth under ideal conditions of fetch limi-
tation or duration limitation, governed by a stationary wind field, can

15

be computed from Hasselmann et al. (1976). For growth along a fetch, the solution yields

$$E_o = 1.6 \times 10^{-7} U^2 \frac{F}{g} \tag{1}$$

and for growth through time, it becomes

$$E_o = 4.3 \times 10^{-10} U^{18/7} g^{-4/7} t^{10/7} \tag{2}$$

where

E_o = total energy resulting from a wind speed U (assumed to be overwater wind conditions adjusted to 33 ft* in elevation), blowing over a given fetch length F

g = acceleration due to gravity

t = total elapsed time since the wind began to blow

28. Two additional pieces of information are required to quantify the distribution of E_o given in the form of an energy density spectrum. The nondimensional peak frequency, $\tilde{f}_m$, and the Phillips' equilibrium constant, α (Phillips 1957), are shown in Figures 3 and 4. Mathematically these parameters are represented by

$$\alpha = 0.076 \tilde{X}^{-0.22} \tag{3}$$

and

$$\tilde{f}_m = 3.5 \tilde{X}^{-0.33} \tag{4}$$

where $\tilde{X}$ is the nondimensional fetch length

$$\tilde{X} = \frac{gF}{U^2} \tag{5}$$

29. The selection of either fetch (Equation 1) or duration

---

* A table of factors for converting U. S. customary units of measurements to metric (SI) units is presented on page 3.
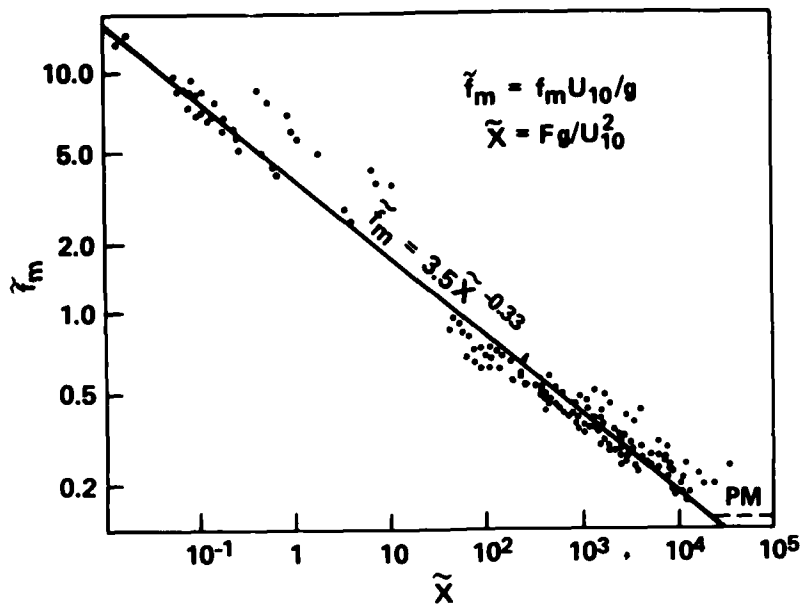
Figure 3. Nondimensional peak frequency $\tilde{f}_m$ as a function of nondimensional fetch length $\tilde{X}$ (after Hasselmann et al. (1973))
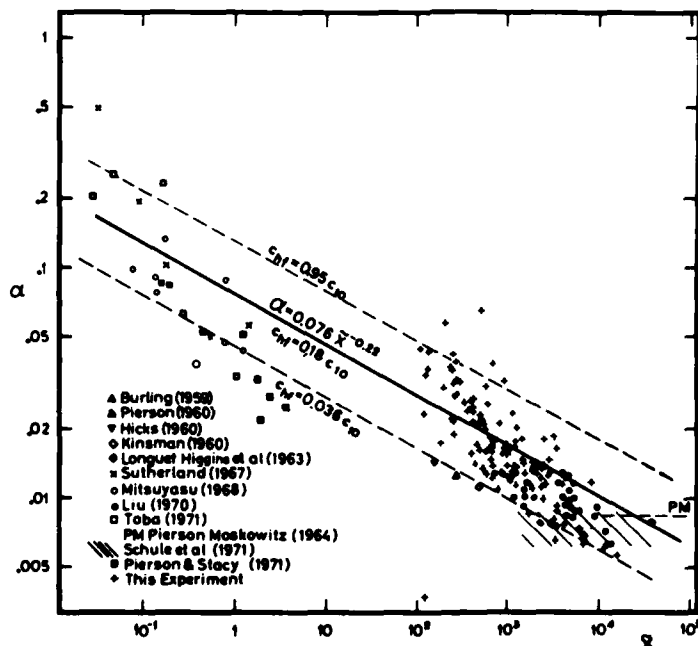
Phillips constant v. fetch scaled according to Kitaigorodskii. Small-fetch data are obtained from wind-wave tanks. (Capillary-wave data was excluded where possible.) Measurements by Sutherland (1967) and Toba (1971) were taken from W.J. Pierson and R.A. Stacy [1973]

Figure 4. Phillips' equilibrium constant α as a function of nondimensional fetch length $\tilde{X}$, after Hasselman et al. (1973)

limited conditions is determined from the following:

$$t_{min} = 5.37 \times 10^2 \left(\frac{U}{g}\right)\left(\frac{gT_s}{U^2}\right)^{7/3} \qquad (6)$$

where

t_{min} = minimum duration condition

T_s = significant wave period (CERC CETN-I-6 1981)

given by:

$$T_s = 7.54 \frac{U}{g} \tanh\left[0.833\left(\frac{g\bar{h}}{U}\right)\right] \tanh\left\{\frac{0.0379\left(\frac{gF}{U^2}\right)^{1/3}}{\tanh\left[0.833\left(\frac{g\bar{h}}{U^2}\right)^{3/8}\right]}\right\} \qquad (7)$$

where $\bar{h}$ is the mean water depth along F.

30. If t_{min} is less than 3 hr (duration of each input wind condition) then Equation 2 will be used to compute the total energy; otherwise, Equation 1 will be employed.

31. The parameterization of the wave growth is somewhat restricted such that when the nondimensional peak frequency attains a value of 0.13 or less, a fully developed sea state is achieved and wave growth is automatically halted. Over long fetch lengths and low wind speeds this condition can occur to some degree of regularity. Thus Equations 1-5 are then redefined by

$$Q = K \sum_{i=1}^{10} \zeta_i \qquad (8)$$

where

Q = the dependent parameters

K = the nonvarying parameters (and constants)

ζ_i = the independent parameters (F and $\tilde{X}$) found in Equations 1-5

The parameter i is the increment counter. After each discrete fetch length F_i, the nondimensional peak frequency is evaluated to determine

18

if $\tilde{f}_m \leq 0.13$. If this occurs, wave growth is curtailed, and wave decay is initiated for the remainder of the fetch length. Wave decay is parameterized following the work conducted by Bretschneider (1952) and Mitsuyasu and Kimura (1965) for f_m (where $f_m = \tilde{f}_m g/U$) while the total energy decay rate follows that described by Jensen (in preparation).

32. Wave conditions generated in Mississippi Sound must also consider dispersion effects resulting from finite water depth conditions. When the water depths vary from F_i to F_{i+1} , one must consider the conservative transformation mechanisms of shoaling and refraction. Wave shoaling is determined from the evaluation of group celerities governed by linear theory. Wave refraction is neglected under the assumptions that: (a) waves travel in the direction of the winds, and more importantly (b) the bottom topography is assumed to be straight and parallel (perpendicular to fetch direction) for every fetch length (discussed in the methodology section). The latter assumption constrains only limited portions of the Mississippi Sound region, where wave propagation can, in its extreme case, travel parallel to the bottom contours. Considering the water depths in Mississippi Sound and peak wave periods ($T = 1/f_m$) in the range of 2 to 8 sec, wave-refraction effects (and subsequent "errors") would be about 2 to 25 percent as shown by the crosshatched area in Figure 5. This is assuming, at most, that the angle between the wave crest and bottom contour is 30 deg. The initial direction of wave propagation is limited to 16 angle classes (because of the wind data employed in this study); thus the accuracy in the resultant refracted wave condition, by similarity, cannot be any more accurate than initially specified. Any differences in the resulting wave climate directional distribution would be minimal.

33. Finite water depth conditions also lead to bottom dissipation effects on the growing seas. Energy losses associated with bottom friction are empirically modeled using the following sets of equations developed by Bretschneider and Reid (1954):

$$E = E_1 \left(\frac{f f E_1 \phi_f \Delta F_i f_m^4}{K_s} \right)^{-1} \tag{9}$$
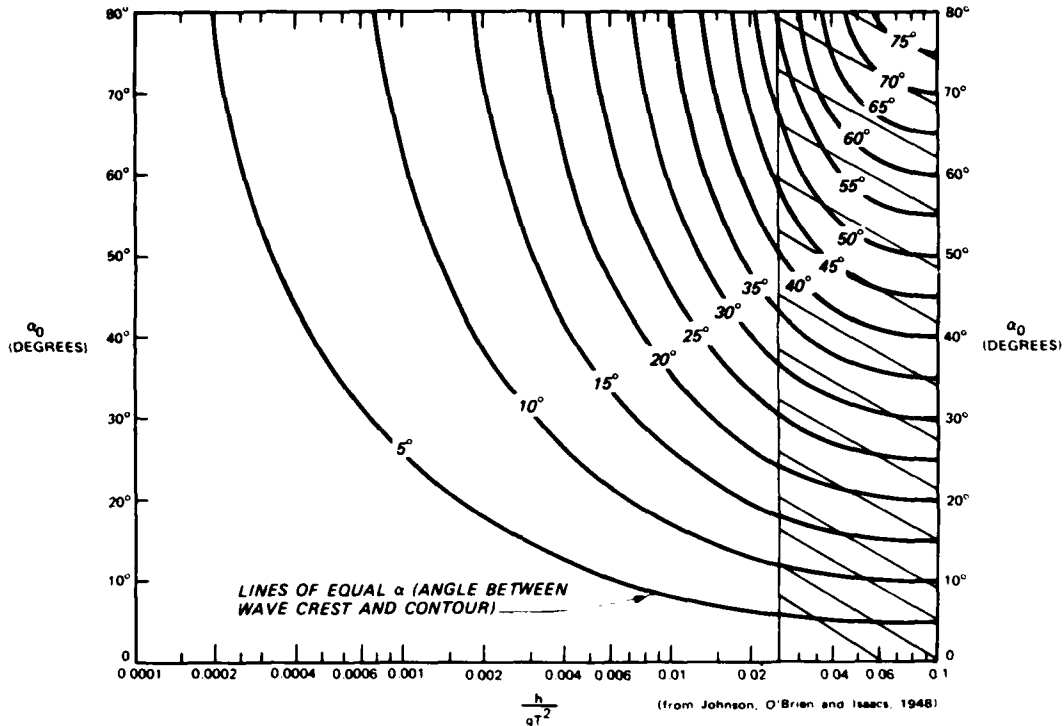
Figure 5. Changes in wave direction due to refraction on slopes with straight and parallel depth contours. The crosshatched area defines the range of wave conditions typically found in Mississippi Sound

where

E = the final total energy at F_i

E_1 = the original total energy at F_{i-1}

ff = the dimensionless friction factor (set for Mississippi Sound at 0.001)

ΔF_i = the distance of wave travel within the discrete fetch length, where

$$K_s = \left\{ \tanh\ (k_i h_i) \left[1 + \frac{2k_i h_i}{\sinh\ (2k_i h_i)} \right] \right\}^{-1/2} \tag{10}$$

and

$$\phi_f = \frac{64\pi^3}{3g^2} \left[\frac{K_s}{\sinh\ (2k_i h_i)} \right]^3 \tag{11}$$

20

where

k_1 = the wave number $(k_i = 2\pi/L_i)$

L_i = the wavelength evaluated for f_m

h_i = the water depth at F_i

34. The second theoretical aspect of SWWM deals primarily with the distribution of the total energy (E_o) in the form of a one-dimensional discrete frequency spectrum $E(f_j)$. Through the use of similarity principles, Kitaigordskii, Kratsitskii, and Zaslavaskii (1975) extended Phillips' deepwater hypothesis (Phillips 1958) of the equilibrium range in the spectrum of wind-generated surface waves to finite depth conditions. The spectral form is defined by

$$E(f_j) = \alpha g^2 (2\pi)^{-4} f_j^{-5} \Phi(\omega_h) \qquad f_j \geq f_m \qquad (12)$$

where

$E(f_j)$ = the energy density at each discrete frequency band, f_j

g = acceleration due to gravity

$\Phi(\omega_h)$ = a nondimensional function dependent on ω_h given by

$$\omega_h = 2\pi f_j \left(\frac{h}{g}\right)^{1/2} \qquad (13)$$

The function $\Phi(\omega_h)$ varies from 1.0 in deep water to 0.0 when $h = 0.0$, as shown by Figure 6. When ω_h is less than 1.0, $\Phi(\omega_h)$ can be approximated by:

$$\Phi(\omega_h) \cong \frac{1}{2} \omega_h^2 \qquad (14)$$

and therefore,

$$E(f_j) = \frac{1}{2} \alpha g h (2\pi)^{-2} f_j^{-3} \qquad f_j \geq f_m \qquad (15)$$

or, the spectral shape changes from an f^{-5} to an f^{-3} in the tail of the energy density spectrum and, more importantly, becomes a function of the water depth.
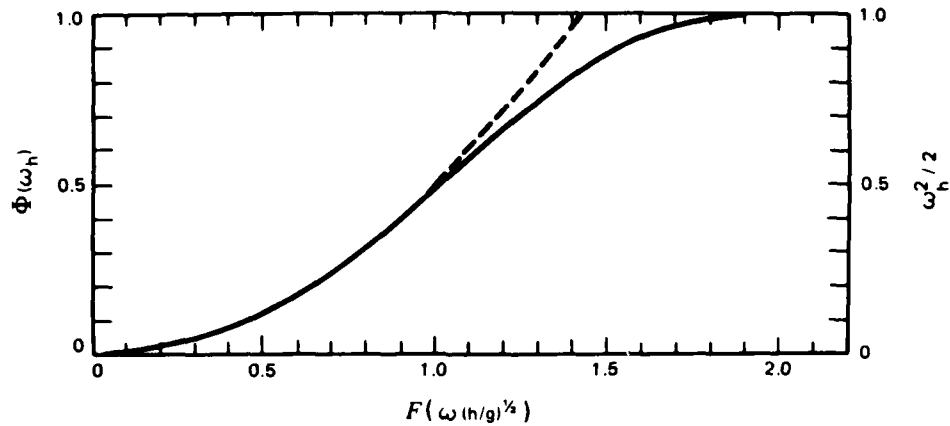
Figure 6. The universal dimensionless function Φ (solid curve) and the function $\omega_h^2/2$ (dashed curve) (after Kitaigordskii, Krasitskii, and Zaslavaskii (1975))

35. The forward face of the spectrum is assumed to be represented by

$$E(f_j) = \alpha g^2 (2\pi)^{-4} f_m^{-5} \exp\left[1 - \left(\frac{f_m}{f}\right)^4\right] \Phi'(\omega_h) \qquad f_j < f_m \qquad (16)$$

where $\Phi'(\omega_h)$ is evaluated from the ω_h defined at f_m. Field and laboratory data by Goda (1974), Thornton (1977), Ou (1980), Iwata (1980), and Vincent (1981) support the form given by Equation 15. The verification of Equation 16 can be found in Vincent[*] and Garcia and Jensen (in preparation).

36. The parametric representation of wave growth assumes a dynamic balance between atmospheric sources and transfers of energy resulting from wave-wave interactions (Figure 2). This parameterization was based on deepwater wave conditions, Hasselmann et al. (1976). During the "Wave Data Acquisition and Hindcast Study for Saginaw Bay" it was determined that over moderately short fetch lengths (10 to 20 nm),

---

[*] C. L. Vincent 1982a. Personal communication, U. S. Army CERC, Fort Belvoir, Va.

this deepwater growth rate expression (Equations 1 and 2) consistently underpredicted the total energy found in the measured data (Garcia and Jensen, in preparation). The only theoretically consistent location to add the energy would be on the forward face of the spectrum (Figure 7). The function $E(f,h)_{THEORY}$ is the saturated spectrum based on Equations 12 and 16, and $E(f,h)_{WEIGHTED}$ is the spectrum based on E_o after wave growth. This process also shifts f_m to a lower frequency which has been noticed in field data (Vincent*). As the fetch length increases, the relative amount of added energy decreases; and eventually, no additional energy is incorporated into the resulting spectrum.

37. It has been shown that the water depth greatly influences the spectral shape and in so doing will influence the maximum wave condition. The parametric formulation follows the work conducted by Vincent (1981). The depth-limiting maximum wave condition is given by,

$$H_m = 4\left[\int_{f_c}^{\infty} E(f) \, df\right]^{1/2} \tag{17}$$

where

H_m = maximum wave condition

f_c = lower frequency bounding the total energy (equal to $0.9f_m$)

$E(f)$ = from Equation 12

Integrating Equation 17, one obtains the absolute limit on the wave condition at a particular water depth, where

$$H_m = \frac{(\alpha gh)^{1/2}}{\pi f_c} \tag{18}$$

38. In summary, the physical process governing wave generation and transformations has been theoretically determined using available, state-of-the-art techniques. It must be emphasized that not all shallow-water

---

* C. L. Vincent 1982b. Personal communication, U. S. Army CERC, Fort Belvoir, Va.
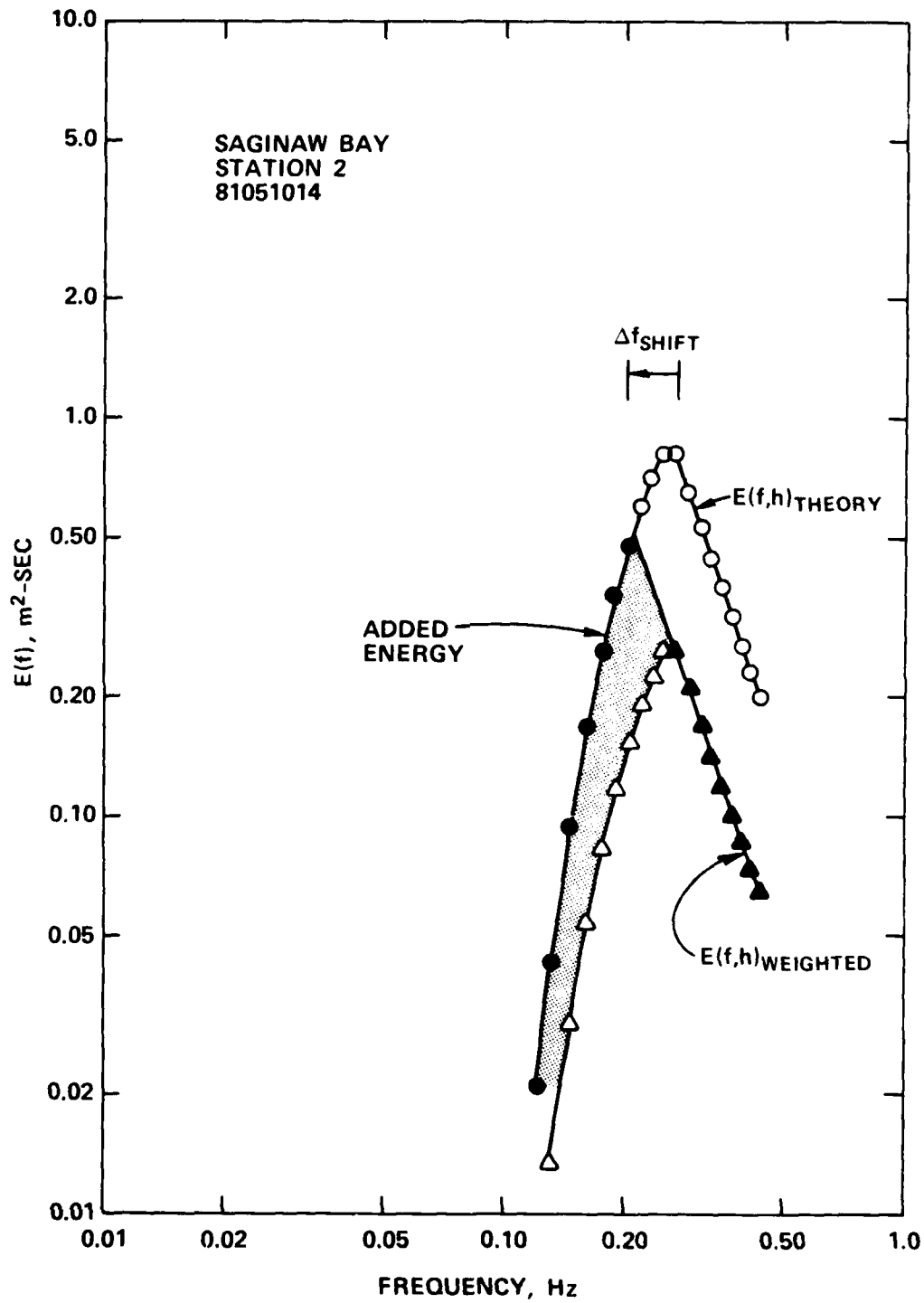
Figure 7. Construction of the final energy density spectrum (solid symbols) caused by shallow-water wave generation

transformation processes have been (or can be) measured to determine their relative effect on the total energy, spectral shape, and peak frequency. Therefore, the development of the SWWM employed in the Mississippi Sound Wave-Hindcast Study attempts to model the physics of the problem in a general sense, while effectively maximizing computational efficiency.

SWWM Setup for Mississippi Sound

39. The SWWM is designed to compute wave conditions at selected locations in Mississippi Sound. All wave conditions generated assume constant water depths over time, therefore neglecting changes in the water elevation caused by tides, freshwater discharges, and surges. In order to improve computational efficiency, a polar coordinate system is selected wherein the origin is placed at each of the 23 selected station locations (Table 3 and Figure 8). Fetch length rays are projected outward from the origin at 20-deg intervals. A total of 18 rays exist for each station. The selection of the 18 rays at 20-deg intervals assures that the variability of the shoreline boundaries (other than 0, 90, 180, and 270 deg) are accurately described rather than using only the 16 wind angle class directions. Fetch lengths and water depths are discretized into 10 subsections along the total length of every ray. The water depth selected for each subsection is interpolated from available NOAA bathmetric charts. The parameters h_i (discrete water depth), F_i (discrete fetch length), and F_t $\left(\text{total fetch length, where } F_t = \sum_{i=1}^{10} F_i\right)$ then become direct functions of a given wind direction. This is shown schematically for Station 1 in Figures 9 and 10. All fetch lengths and water depths are tabulated in Appendix C. Special fetch lengths are provided for certain station locations when the given wind direction is either 90-deg or 270-deg azimuth (see Appendix C). In many instances the wind direction will not correspond identically to a given fetch length ray. When this occurs, a new $F_t(\theta_w)$ and $h_i(F_i,\theta_w)$ are computed via linear interpolation between two discrete fetch length rays.

25

Table 3

Station Locations and Water Depths

Station No.	Longitude, W deg	Latitude, N deg	Water Depth ft
1	88.17	30.28	6.5
2	88.25	30.28	9.5
3	88.30	30.20	12.0
4	88.30	30.25	16.5
5	88.42	30.25	17.0
6	88.50	30.25	19.0
7	88.58	30.25	10.0
8	88.58	30.32	8.0
9	88.67	30.29	13.0
10	88.75	30.29	11.5
11	88.83	30.33	9.0
12	88.83	30.25	15.0
13	88.92	30.33	11.0
14	88.92	30.25	15.0
15	89.00	30.33	10.5
16	89.00	30.25	16.0
17	89.08	30.33	9.0
18	89.08	30.26	15.0
19	89.17	30.29	13.0
20	89.25	30.25	9.0
21	89.25	30.17	12.5
22	89.33	30.21	11.0
23	89.33	30.15	11.0

26
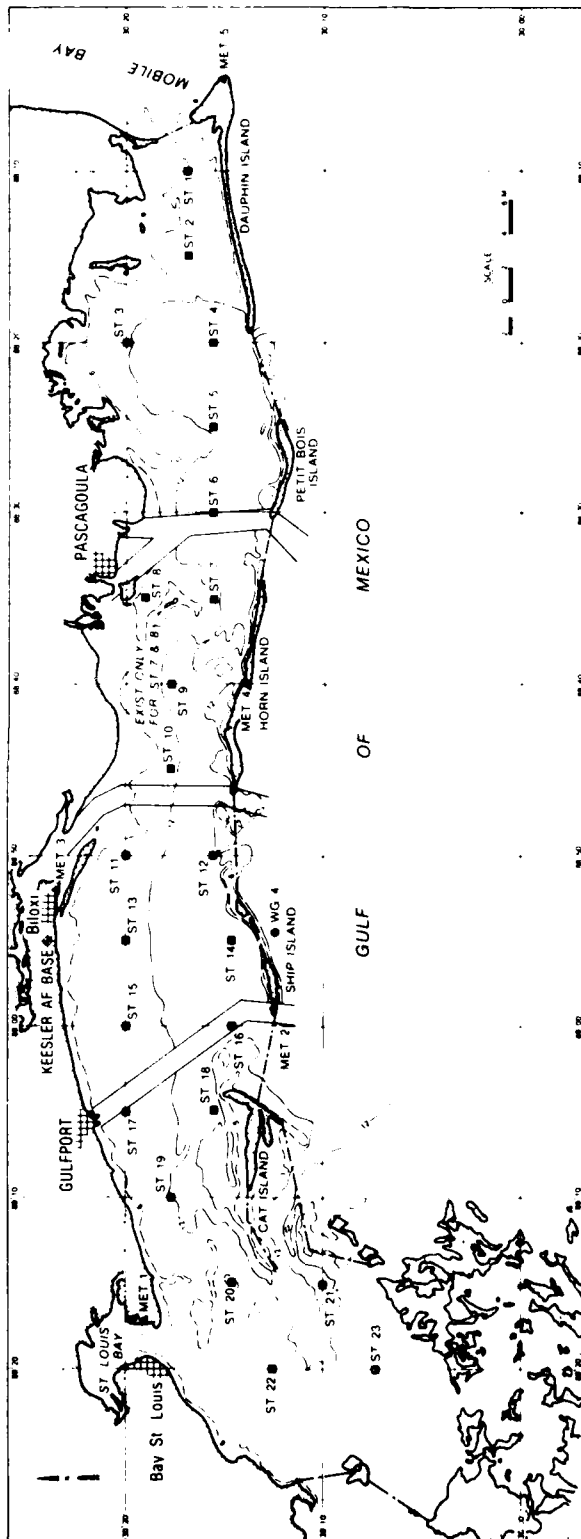
Figure 8. Mississippi Sound wave-hindcast station locations
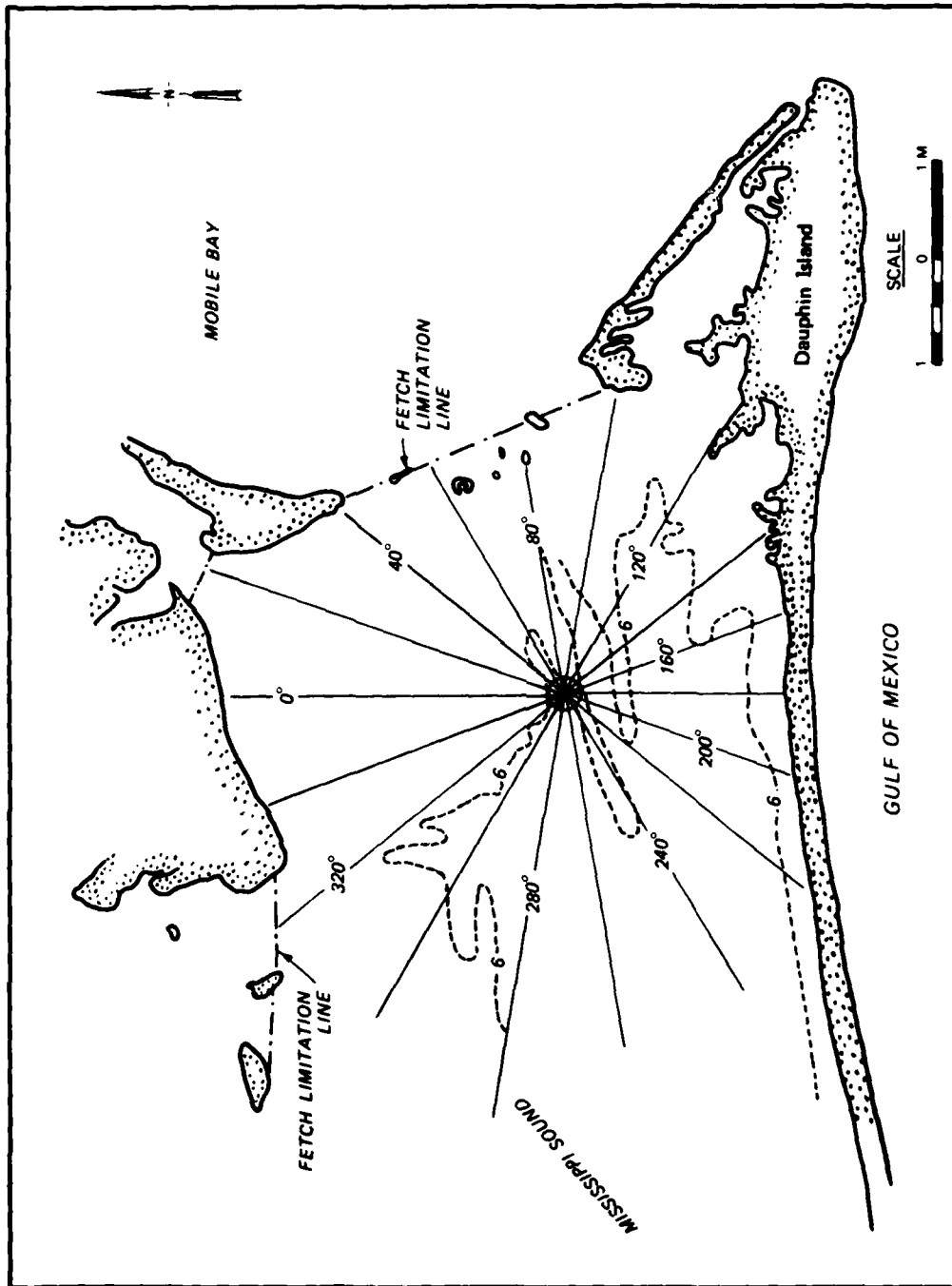
Figure 9. Schematic representation of the polar coordinate system employed in the
Mississippi Sound Wave-Hindcast Study
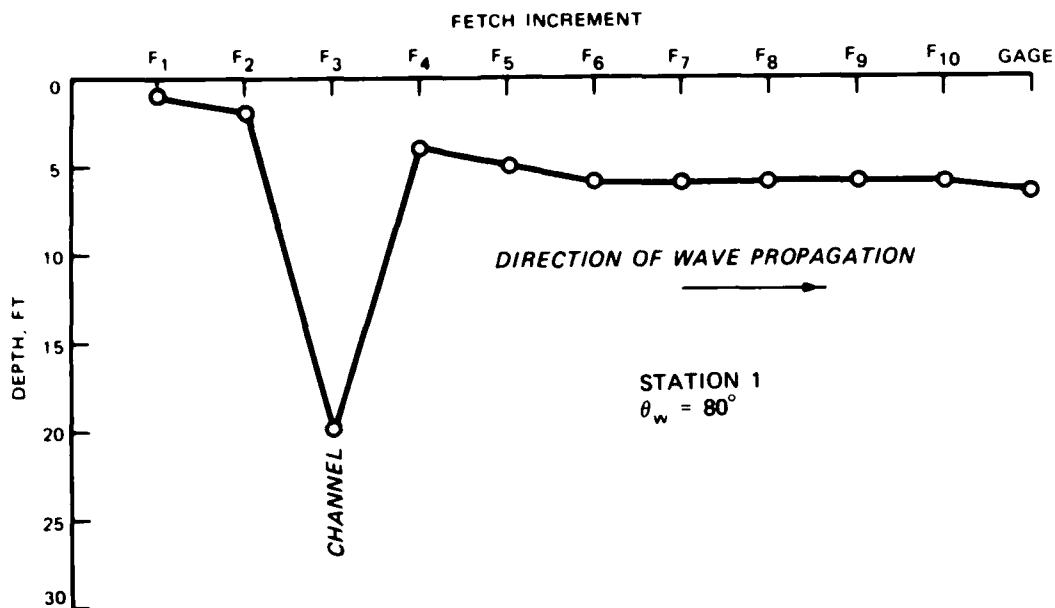
Figure 10. Schematic representation of the discrete water depths as a function of wind direction

40. For the shallow-water wave spectrum $E(f_j)$ defined in the previous section, 35 frequency bands are selected that will adequately describe the energy distribution. The frequency bands range from 0.083 to 2.0 Hz and are tabulated in Appendix C. Since $\Phi(\omega_n)$ (Equations 12 and 16) is dependent on each discrete frequency and the water depth at a given station location, all values were then precomputed and stored on file to be used later in the computational scheme.

41. The input conditions to the SWWM are the wind speed (given at 33 ft measured overland) and the wind direction (measured "from-which-they-came," in degrees azimuth). The wind speed is then adjusted to overwater winds as previously discussed in PART II. The proper fetch length, F_t , and water depths, h_i , are then selected for each station for the given wind direction. With this information, the SWWM is now ready to compute the wave conditions throughout Mississippi Sound. This procedure is followed for every 3-hr interval over the 20-year period of record.

42. With all dependent parameters known $\left(\theta_w, \ F_t(\theta_w), \ h_i(F_i, \ \theta_w) \right)$

wave growth can be initiated. The first step in the growth sequence
selects either duration or fetch-limited conditions. From that point,
total energy growth is dependent on a discrete increment of time (t_i) or
fetch length (F_i). Wave transformation processes then act only on the
portion of energy created in a given fetch (or time) increment. Changes
in the group speed $C_{g_i}(h_i, f_m)$ are determined from the changes in
water depth from F_{i-1} to F_i, and assuming f_m remains constant.
Energy losses associated with bottom friction effects are also treated
in a similar manner. Figure 11 schematized the processes involved in
fetch-limited energy growth. Duration-limited energy growth follows the
same procedure where temporal growth rates are employed. When satura-
tion conditions exist $(\tilde{f}_m \leq 0.13)$, energy growth will terminate and the
energy will be decayed. During the latter sequence, the transformation
processes will continue to act on the residual energy (E_{RES}) following
the previously described procedure.

43. Once E_o is determined, it now becomes a matter of distrib-
uting that energy over $E(f_j)$. This is performed at each station, em-
ploying a slightly modified version of Equations 12-16. Integrating
$E(f_j, h_s)$, now dependent on the water depth at a given station (h_s),
one finds the total saturated energy caused by a given wind condition
blowing over a fetch length for some period of time:

$$E_{o_{SAT}} = \int_0^\infty E(f_j, h_s)\, df \qquad (19)$$

Therefore, the resulting spectrum $E^*(f_j, h_s)$ is then scaled according
to E_o (the total available energy). Hence,

$$E^*(f_j, h_s) = \gamma E(f_j, h_s) \qquad (20)$$

where γ is equal to $E_o/E_{o_{SAT}}$.

44. The resulting spectrum $E^*(f_j, h_s)$ is then readjusted to
compensate for employing a deepwater parametric form of energy growth.
The procedure follows the technique described earlier in this section.
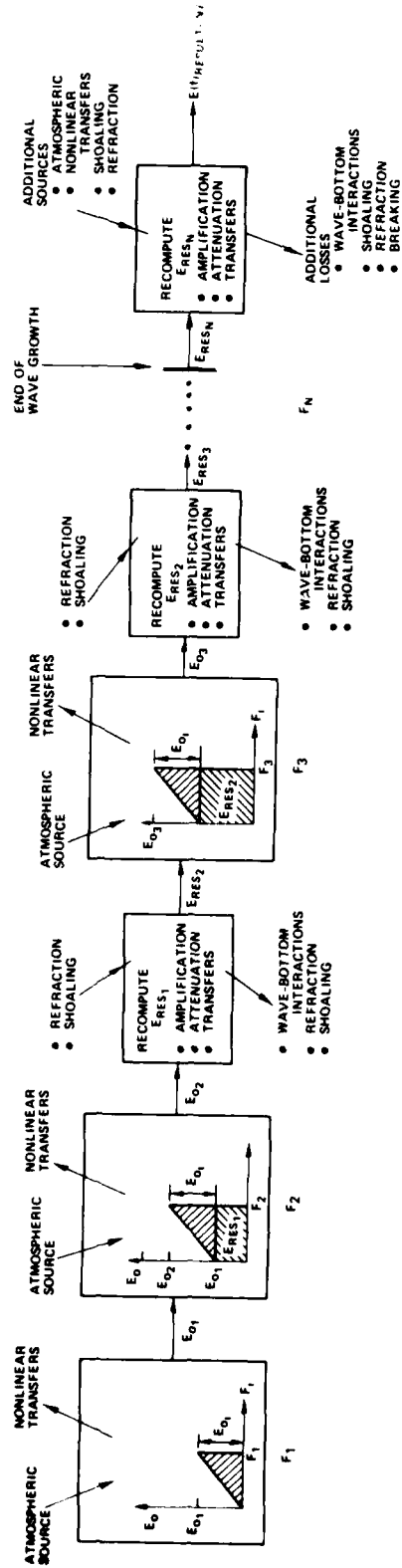
Figure 11. Schematic representation of the methodology associated with the shallow-water wave modeling technique

If conditions are such that the total energy is decaying during wave growth, this step is neglected. Thus, at this point in the SWWM, a one-dimensional discrete energy density spectrum is provided for each of the 23 stations for one 3-hr period.

45. The wave parameters are computed by

$$H_s = 4 \left[\int_0^\infty E^*(f_j, h_s) \, df \right]^{1/2} \tag{21}$$

and

$$T = \frac{1}{f_m} \tag{22}$$

where f_m is equal to f_j, where the maximum energy density occurs. The direction of wave propagation ψ is assumed to be equal to the wind direction for all stations.

46. A final check is made to determine if H_s (Equation 21) is greater than H_m (Equation 18). If $H_s > H_m$, then $E^*(f_j, h_s)$ must be scaled according to H_m similar to Equation 20, where γ now equals $\left(H_m^2 / H_s^2 \right)$.

Calibration and Verification

47. In all wave hindcasting studies, comparisons to actual gage measurements are necessary to determine the validity of the long-term wave statistics. It is unfortunate that ship observations and wave gage data in Mississippi Sound are very limited. In a search of 20 years of ship observation records, only 27 records were obtained. Although a wave gaging program was performed by Raytheon Ocean Systems Company as part of the Mississippi Sound Data Collection Program, only one of the two wave data sets prepared was acceptable for comparisons to the SWWM results.

48. The SWWM results are compared with the limited ship records during the period of 3-10 March 1965 (Figure 12). It should be noted that measured data are incremented in 0.5-m intervals and the location

32
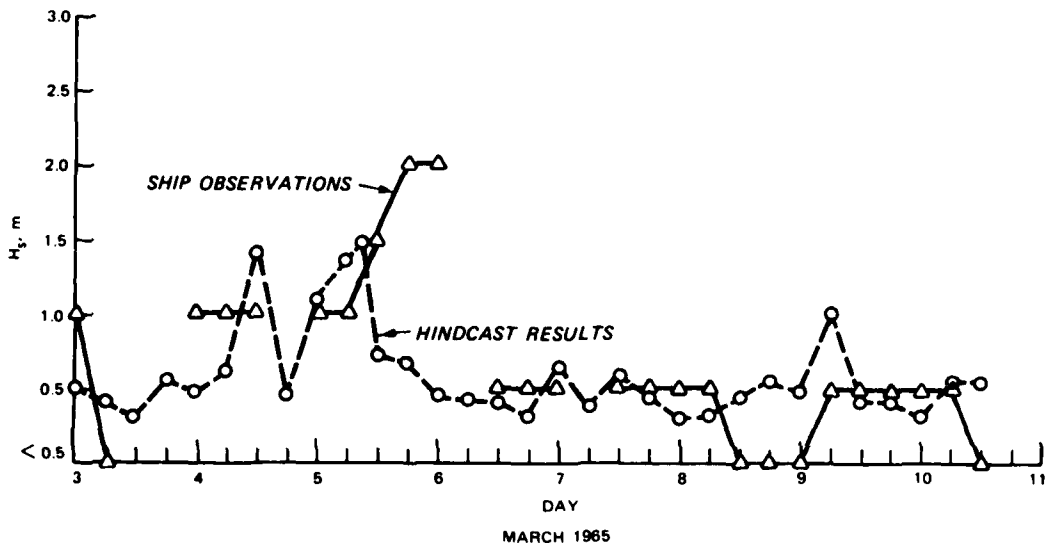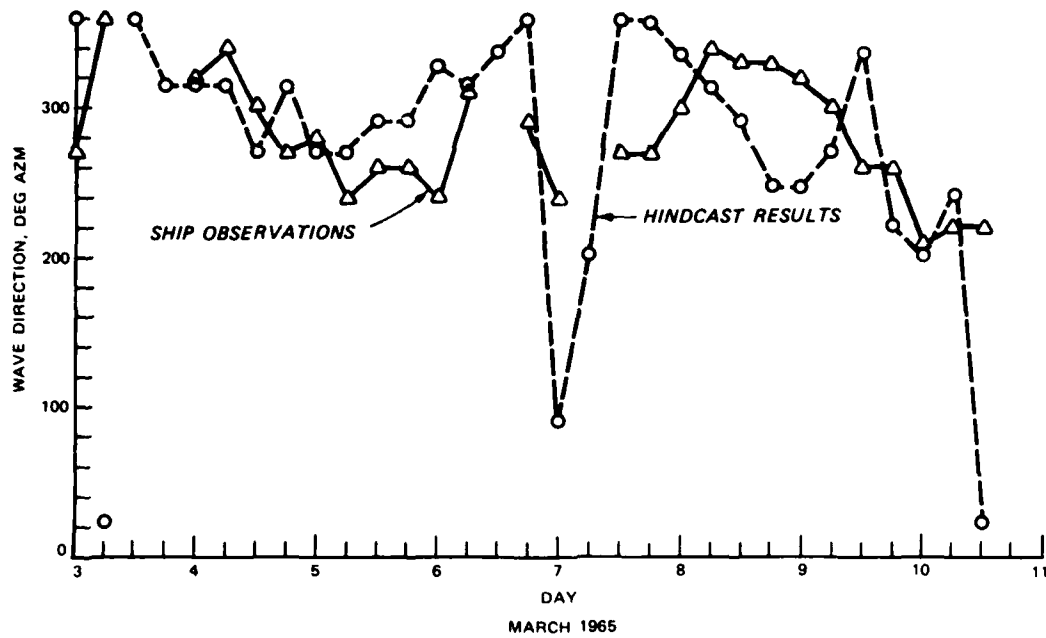
Figure 12. Comparison of ship observation and hindcast results for direction of wave propagation (ψ) and significant height (H_s)

33

of the ship is available only to the nearest 0.1 deg. Both of these factors make one-to-one comparisons difficult. Overall, the SWWM results display similar trends observed in the ships records for both ψ and H_s.

49. As mentioned, the wave gaging program involved in the Mississippi Sound reconnaissance study (USAED, Mobile, 1981) had limited success. Review of the wave gage operations revealed that the gage could not resolve wave periods less than 5.0 sec. Since Roberts* concluded that 61 to 71 percent of the waves south of Mississippi Sound have wave periods of less than 5.0 sec and since the gage could not resolve these conditions, comparisons of hindcast and gage-measured wave periods are not appropriate for verification.

50. The only station at which suitable prototype measurements of wave height are available is actually outside of Mississippi Sound just south of Ship Island (Figure 8, WG 4). Comparisons of hindcast and gage-measured H_s are presented in Figure 13. The hindcast H_s data follow the trends of the recorded data with slight phase shifts between the two data sets. If the phasing were adjusted, the differences between the data would be about ±0.5 ft.

51. Although the H_s comparisons indicate good agreement between the hindcast and measured data, extensive comparisons were not performed due to the problem of the gage-measured wave period. Without the wave period comparisons, the gage-measured wave data are not appropriate for use in verifying the SWWM.

52. In order to provide a more detailed verification of the SWWM, additional comparisons between the SWWM and measured wave data are shown in Appendix A. The data are obtained from a similar hindcast study in Saginaw Bay, Michigan. The methodology of the SWWM is consistent with the Mississippi Sound study and Saginaw Bay. The primary purpose for that study was verification of the SWWM with wave gage data. Differences between the two data sets are ±0.5 ft for H_s and ±1.0 sec for T

---

* N. C. Roberts. 1974. "Wave Height Statistics, Mississippi," Nash C. Roberts, Jr., Consultants (typewritten report).
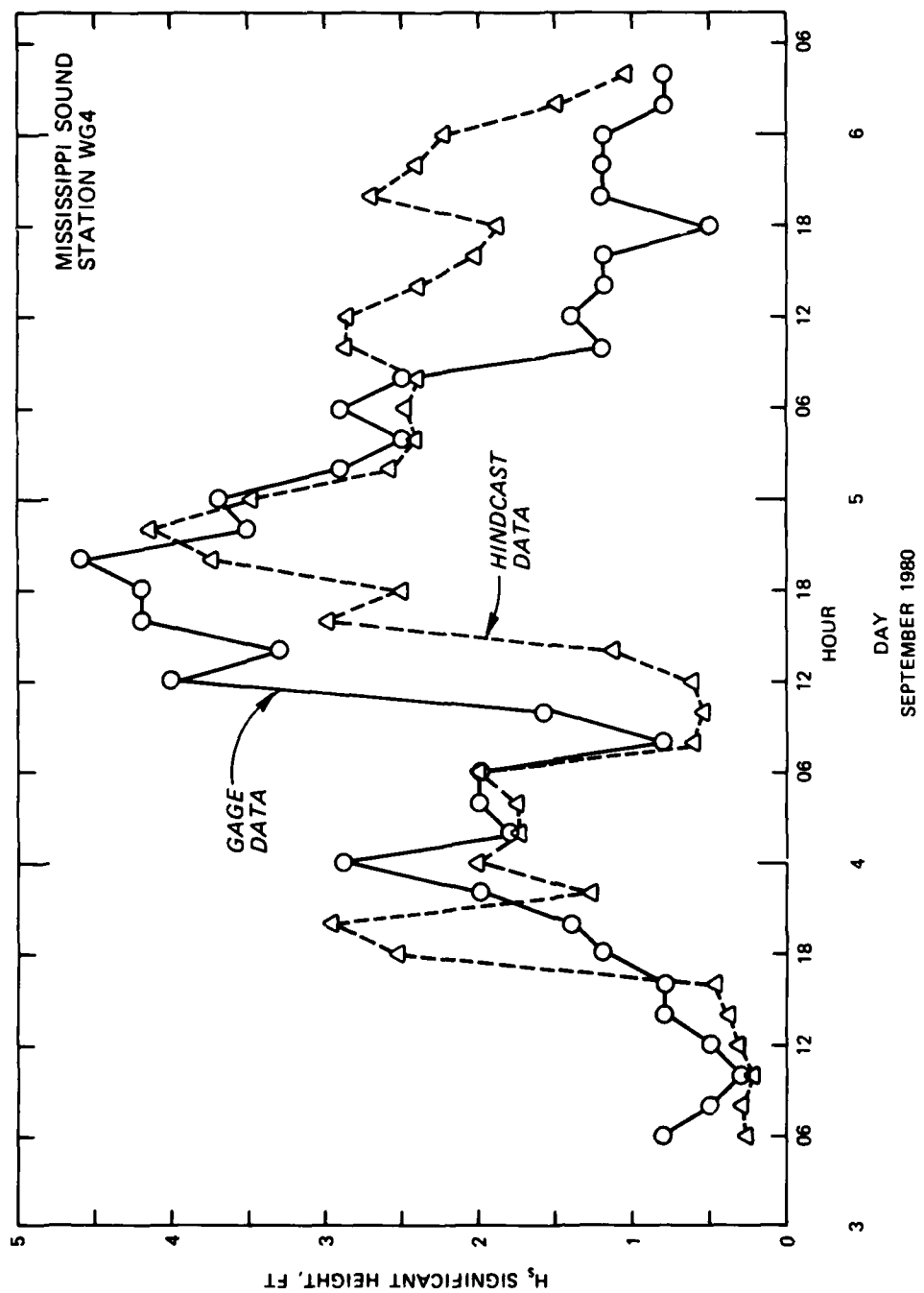
Figure 13. Comparison of measured and hindcast significant wave-height data (Station 4 location is found in Figure 8, identified as WG 4)

35

(Garcia and Jensen, in preparation). These "error bands" associated with the hindcast results are expected to apply to the results of the Mississippi Sound study; but without additional field data (in the Sound), these confidence limits cannot be taken as definitive.

PART IV: 20-YEAR HINDCAST RESULTS

53. This section of the report is intended only to serve as a general description of simple wave characteristics such as height, period, and direction of wave propagation. More detailed analysis of one-dimensional spectral properties and interrelations among various wave parameters related to storm characteristics cannot be covered in the scope of this report.*

54. The 20-year hindcast only considers a single population of wave conditions defined as sea (although during peiods of time, the non-dimensional peak frequency is less than 0.13, defined as swell by Hassel-mann et al. (1976)). Also, all wind data are assumed to be derived from extratropical storm conditions; therefore wave characteristics calculated for periods of tropical storms (Table 2) must be regarded as approximate. Any extremal analysis of H_s based cn these data will probably result in an underestimate of H_s conditions. All water depths employed in this study were assumed to be constant, neglecting tides and surges.

55. The wave parameters H_s (Equation 20), T (Equation 21), and ψ given at each station every 3 hr for 20 years are used as a basis to construct all products found in Appendices D-G. The value of the wave direction is the direction from which the waves are coming (Figure 14). Azimuths are measured clockwise in degrees from true north (0). As previously mentioned, the direction of wave propagation is limited to 16 categories (22.5-deg increments from 0 deg to 337.5 deg).

56. Six products are presented:

   a. Seasonal and 20-year Percent Occurrence Tables.

   b. Percent Exceedance Diagrams.

   c. Height, Period, and Direction Histograms.

   d. Mean H_s and Largest H_s Tables.

   e. "Over" Duration Tables.

   f. "Under" Duration Tables.

---

* One-dimensional frequency spectra and H_s, T, and ψ are stored at 3-hr intervals for 20 years for each station.

WAVE DIRECTION
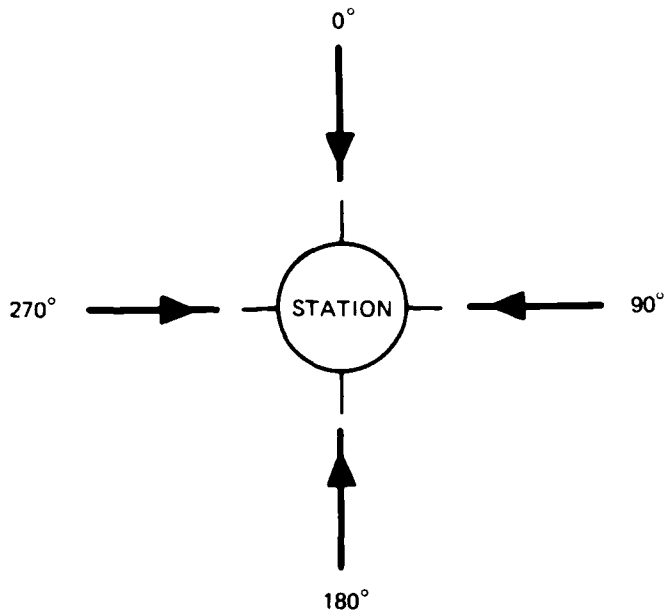
Figure 14. Diagram indicating wave directions

A brief description of each product is given and sections on use of the products, including examples, are provided. Each product, except the duration tables (Appendices F and G), is provided separately for each station. The duration tables for waves over and under specified wave heights are presented in two tabulations, each incorporating all stations.

Seasonal and 20-Year Percent Occurrence Tables

Description

57. Two types of tables are printed: azimuth tables and all-directions tables. The azimuth tables (Figure 15) give the percent occurrence of significant waves in height and period ranges for specified

STATION 1 SEASON 1   ANGLE CLASS (DEG AZIMUTH)= 0.
WATER DEPTH = 6.50 FEET
PERCENT OCCURRENCE(X1000) OF HEIGHT AND PERIOD BY DIRECTION

HEIGHT(FEET)	0.0-0.9	1.0-1.9	3.0-2.9	3.0-3.9	4.0-4.9	5.0-5.9	6.0-6.9	7.0-7.9	8.0-8.9	9.0-LONGER	TOTAL
0. - 0.49	.	1585	4632	.	.	.	.	.	.	.	6217
0.50 - 0.99	.	.	7112	270	.	.	.	.	.	.	7382
1.00 - 1.49	.	.	.	297	.	.	.	.	.	.	297
1.50 - 1.99	.	.	.	.	.	.	.	.	.	.	0
2.00 - 2.49	.	.	.	.	.	.	.	.	.	.	0
2.50 - 2.99	.	.	.	.	.	.	.	.	.	.	0
3.00 - 3.49	.	.	.	.	.	.	.	.	.	.	0
3.50 - 3.99	.	.	.	.	.	.	.	.	.	.	0
4.00 - 4.49	.	.	.	.	.	.	.	.	.	.	0
4.50 - 4.99	.	.	.	.	.	.	.	.	.	.	0
5.00 - GREATER	.	.	.	.	.	.	.	.	.	.	0
TOTAL	0	1585	11744	567	0	0	0	0	0	0	

AVERAGE HS(FT) = 0.54   LARGEST HS(FT) = 1.30   ANGLE CLASS % = 13.9

STATION 1 SEASON 1   ANGLE CLASS (DEG AZIMUTH)= 22.5
WATER DEPTH = 6.50 FEET
PERCENT OCCURRENCE(X1000) OF HEIGHT AND PERIOD BY DIRECTION

HEIGHT(FEET)	0.0-0.9	1.0-1.9	3.0-2.9	3.0-3.9	4.0-4.9	5.0-5.9	6.0-6.9	7.0-7.9	8.0-8.9	9.0-LONGER	TOTAL
0. - 0.49	.	394	3192	.	.	.	.	.	.	.	3586
0.50 - 0.99	.	.	2659	207	.	.	.	.	.	.	2866
1.00 - 1.49	.	.	.	110	.	.	.	.	.	.	110
1.50 - 1.99	.	.	.	.	.	.	.	.	.	.	0
2.00 - 2.49	.	.	.	.	.	.	.	.	.	.	0
2.50 - 2.99	.	.	.	.	.	.	.	.	.	.	0
3.00 - 3.49	.	.	.	.	.	.	.	.	.	.	0
3.50 - 3.99	.	.	.	.	.	.	.	.	.	.	0
4.00 - 4.49	.	.	.	.	.	.	.	.	.	.	0
4.50 - 4.99	.	.	.	.	.	.	.	.	.	.	0
5.00 - GREATER	.	.	.	.	.	.	.	.	.	.	0
TOTAL	0	394	5851	317	0	0	0	0	0	0	

AVERAGE HS(FT) = 0.52   LARGEST HS(FT) = 1.18   ANGLE CLASS % = 6.6

STATION 1 SEASON 1   ANGLE CLASS (DEG AZIMUTH)= 45.0
WATER DEPTH = 6.50 FEET
PERCENT OCCURRENCE(X1000) OF HEIGHT AND PERIOD BY DIRECTION

HEIGHT(FEET)	0.0-0.9	1.0-1.9	3.0-2.9	3.0-3.9	4.0-4.9	5.0-5.9	6.0-6.9	7.0-7.9	8.0-8.9	9.0-LONGER	TOTAL
0. - 0.49	.	2957	3220	.	.	.	.	.	.	.	6177
0.50 - 0.99	.	.	1502	.	.	.	.	.	.	.	1502
1.00 - 1.49	.	.	.	6	.	.	.	.	.	.	6
1.50 - 1.99	.	.	.	.	.	.	.	.	.	.	0
2.00 - 2.49	.	.	.	.	.	.	.	.	.	.	0
2.50 - 2.99	.	.	.	.	.	.	.	.	.	.	0
3.00 - 3.49	.	.	.	.	.	.	.	.	.	.	0
3.50 - 3.99	.	.	.	.	.	.	.	.	.	.	0
4.00 - 4.49	.	.	.	.	.	.	.	.	.	.	0
4.50 - 4.99	.	.	.	.	.	.	.	.	.	.	0
5.00 - GREATER	.	.	.	.	.	.	.	.	.	.	0
TOTAL	0	2957	4722	6	0	0	0	0	0	0	

AVERAGE HS(FT) = 0.36   LARGEST HS(FT) = 1.05   ANGLE CLASS % = 7.7

STATION 1 SEASON 1   ANGLE CLASS (DEG AZIMUTH)= 67.5
WATER DEPTH = 6.50 FEET
PERCENT OCCURRENCE(X1000) OF HEIGHT AND PERIOD BY DIRECTION

HEIGHT(FEET)	0.0-0.9	1.0-1.9	3.0-2.9	3.0-3.9	4.0-4.9	5.0-5.9	6.0-6.9	7.0-7.9	8.0-8.9	9.0-LONGER	TOTAL
0. - 0.49	.	2998	1530	.	.	.	.	.	.	.	4528
0.50 - 0.99	.	.	747	.	.	.	.	.	.	.	747
1.00 - 1.49	.	.	.	.	.	.	.	.	.	.	0
1.50 - 1.99	.	.	.	.	.	.	.	.	.	.	0
2.00 - 2.49	.	.	.	.	.	.	.	.	.	.	0
2.50 - 2.99	.	.	.	.	.	.	.	.	.	.	0
3.00 - 3.49	.	.	.	.	.	.	.	.	.	.	0
3.50 - 3.99	.	.	.	.	.	.	.	.	.	.	0
4.00 - 4.49	.	.	.	.	.	.	.	.	.	.	0
4.50 - 4.99	.	.	.	.	.	.	.	.	.	.	0
5.00 - GREATER	.	.	.	.	.	.	.	.	.	.	0
TOTAL	0	2998	2277	0	0	0	0	0	0	0	

AVERAGE HS(FT) = 0.31   LARGEST HS(FT) = 0.95   ANGLE CLASS % = 5.3

Figure 15.   Sample percent occurrence tables by season and direction

station, season,* and direction. The title of each table identifies the station, season, angle class, and water depth. The wave period ranges are in 1-sec intervals and the height ranges are in 1/2-ft increments. Values in the azimuth tables represent the percent of the season that waves occur from the specified angle class for the indicated height and period ranges. The values have been multiplied by 1,000 to allow more accuracy with less printing space. Summations of period and height ranges are provided in the last column and row of each table. The summations are also multiplied by 1,000. The last line in each directional table contains the following information for the specified angle class and season:

    <u>a</u>. The average H_s .

    <u>b</u>. The largest H_s .

    <u>c</u>. Percent of waves occurring in the specified season from the indicated angle class.

58. The all-directions table for each season (Figure 16) is printed after the 337.5-deg angle class table for the specified season. These tables give the percent occurrence of significant waves within the same specified height and period ranges coming from all directions for the indicated season and station. Values in the all-directions tables

```
                   STATION   1   SEASON  1      FOR ALL DIRECTIONS
              WATER DEPTH =  6.50  FEET
              PERCENT OCCURRENCE(X100) OF HEIGHT AND PERIOD FOR ALL DIRECTIONS
HEIGHT(FEET)                               PERIOD(SECONDS)                              TOTAL

              0.0-  1.0-  3.0-  3.0-  4.0-  5.0-  6.0-  7.0-  8.0-  9.0-
              0.9   1.9   2.9   3.9   4.9   5.9   6.9   7.9   8.9   LONGER

0.00 - 0.49     .   2556  3007    21    .     .     .     .     .     .       5584
0.50 - 0.99     .     .   3202   299    51    48    85     .     .     .       3665
1.00 - 1.49     .     .      9   236    70     .    45     .     .     .        360
1.50 - 1.99     .     .      .     3    69     .     .     .     .     .         72
2.00 - 2.49     .     .      .     .     4     .     .    83     .     .         87
2.50 - 2.99     .     .      .     .     .     .     .    17    40    10         67
3.00 - 3.49     .     .      .     .     .     .     .     .     .     6          6
3.50 - 3.99     .     .      .     .     .     .     .     .     .     .          0
4.00 - 4.49     .     .      .     .     .     .     .     .     .     .          0
4.50 - 4.99     .     .      .     .     .     .     .     .     .     .          0
5.00 - GREATER  .     .      .     .     .     .     .     .     .     .          0
     TOTAL      0   2556  6218   559   194    48   130   100    40    16

   AVE HS(FT) = 0.51    LARGEST HS(FT) = 3.19    TOTAL CASES = 14440.
```

Figure 16. Sample percent occurrence table for one season and all directions

---

* Season 1 is December through February, Season 2 is March through May, Season 3 is June through August, and Season 4 is September through November.

are multiplied by 100. The parameters listed in the last line of the seasonal tables are derived from all directions of the specified season. The number of cases represents the number of wave conditions occurring in the indicated season for the total 20 years analyzed. All calm wave conditions ($H_s < 0.1$ ft) are removed from these tables because of the methodology employed in the SWWM. This constraint will not alter the data since: (a) we are dealing with a very small number of occurrences within a given period of time, and (b) the magnitude of H_s is so small that whether one considers a wave height of 0.1 ft or 0.0 ft is of no real consequence.

59. The 20-year tables (Figures 17 and 18) also included in this report are of the same format described above. These tables (angle class tables and all-directions tables) are based on the full 20-year data set (or the cumulative total of the four sets of seasonal tables).

Use of the tables

60. The tables have been developed to produce reliable information when seasonal or 20-year intervals are employed.

Examples

61. In order to find the number of hours that waves of ≥ 1.0 ft and ≤ 1.5 ft and 3.0 to 3.9 sec are expected to occur from 45 deg at Station 1 in Season 1 (December, January, February) for a 20-year interval, the value read in the table for the specified station, season, angle class, height, and period should first be divided by 1,000, which for this example yields 0.006 percent (Figure 15, Appendices D and E). Then 0.006 is divided by 100 to give the probability, and multiplied by the number of hours in Season 1 for the 20-year interval to yield the number of hours that the specified wave is expected to occur. The simple conversion process is:

$$\frac{\text{value read in table}}{1,000} \div 100 \times \begin{array}{l}\text{number of} \\ \text{hours in} \\ \text{time interval}\end{array} = \begin{array}{l}\text{number of hours} \\ \text{specified wave is} \\ \text{expected to occur}\end{array} \quad (25)$$

For this example:

$$\frac{6}{1,000} \div 100 \times 43{,}320 \cong 3 \text{ hr}$$

41

STATION 1 20 YEARS ANGLE CLASS (DEG AZIMUTH) = 0.
WATER DEPTH = 6.50 FEET
PERCENT OCCURRENCE(X1000) OF HEIGHT AND PERIOD BY DIRECTION

HEIGHT(FEET)	PERIOD(SECONDS)										TOTAL
	0.0-0.9	1.0-1.9	2.0-2.9	3.0-3.9	4.0-4.9	5.0-5.9	6.0-6.9	7.0-7.9	8.0-8.9	9.0-LONGER	
0. - 0.49	.	2082	4122	.	.	.	.	.	.	.	6204
0.50 - 0.99	.	.	3973	102	.	.	.	.	.	.	4075
1.00 - 1.49	.	.	.	135	.	.	.	.	.	.	135
1.50 - 1.99	.	.	.	1	.	.	.	.	.	.	1
2.00 - 2.49	.	.	.	.	.	.	.	.	.	.	0
2.50 - 2.99	.	.	.	.	.	.	.	.	.	.	0
3.00 - 3.49	.	.	.	.	.	.	.	.	.	.	0
3.50 - 3.99	.	.	.	.	.	.	.	.	.	.	0
4.00 - 4.49	.	.	.	.	.	.	.	.	.	.	0
4.50 - 4.99	.	.	.	.	.	.	.	.	.	.	0
5.00 - GREATER	.	.	.	.	.	.	.	.	.	.	0
TOTAL	0	2082	8095	238	0	0	0	0	0	0	

AVERAGE HS(FT) = 0.47   LARGEST HS(FT) = 1.64   ANGLE CLASS % = 10.4

STATION 1 20 YEARS ANGLE CLASS (DEG AZIMUTH) = 22.5
WATER DEPTH = 6.50 FEET
PERCENT OCCURRENCE(X1000) OF HEIGHT AND PERIOD BY DIRECTION

HEIGHT(FEET)	PERIOD(SECONDS)										TOTAL
	0.0-0.9	1.0-1.9	2.0-2.9	3.0-3.9	4.0-4.9	5.0-5.9	6.0-6.9	7.0-7.9	8.0-8.9	9.0-LONGER	
0. - 0.49	.	573	3374	.	.	.	.	.	.	.	3947
0.50 - 0.99	.	.	1767	99	.	.	.	.	.	.	1866
1.00 - 1.49	.	.	.	46	.	.	.	.	.	.	46
1.50 - 1.99	.	.	.	.	.	.	.	.	.	.	0
2.00 - 2.49	.	.	.	.	.	.	.	.	.	.	0
2.50 - 2.99	.	.	.	.	.	.	.	.	.	.	0
3.00 - 3.49	.	.	.	.	.	.	.	.	.	.	0
3.50 - 3.99	.	.	.	.	.	.	.	.	.	.	0
4.00 - 4.49	.	.	.	.	.	.	.	.	.	.	0
4.50 - 4.99	.	.	.	.	.	.	.	.	.	.	0
5.00 - GREATER	.	.	.	.	.	.	.	.	.	.	0
TOTAL	0	573	5141	145	0	0	0	0	0	0	

AVERAGE HS(FT) = 0.45   LARGEST HS(FT) = 1.21   ANGLE CLASS % = 5.9

STATION 1 20 YEARS ANGLE CLASS (DEG AZIMUTH) = 45.0
WATER DEPTH = 6.50 FEET
PERCENT OCCURRENCE(X1000) OF HEIGHT AND PERIOD BY DIRECTION

HEIGHT(FEET)	PERIOD(SECONDS)										TOTAL
	0.0-0.9	1.0-1.9	2.0-2.9	3.0-3.9	4.0-4.9	5.0-5.9	6.0-6.9	7.0-7.9	8.0-8.9	9.0-LONGER	
0. - 0.49	.	4062	3347	.	.	.	.	.	.	.	7409
0.50 - 0.99	.	.	1148	.	.	.	.	.	.	.	1148
1.00 - 1.49	.	.	.	1	.	.	.	.	.	.	1
1.50 - 1.99	.	.	.	.	.	.	.	.	.	.	0
2.00 - 2.49	.	.	.	.	.	.	.	.	.	.	0
2.50 - 2.99	.	.	.	.	.	.	.	.	.	.	0
3.00 - 3.49	.	.	.	.	.	.	.	.	.	.	0
3.50 - 3.99	.	.	.	.	.	.	.	.	.	.	0
4.00 - 4.49	.	.	.	.	.	.	.	.	.	.	0
4.50 - 4.99	.	.	.	.	.	.	.	.	.	.	0
5.00 - GREATER	.	.	.	.	.	.	.	.	.	.	0
TOTAL	0	4062	4495	1	0	0	0	0	0	0	

AVERAGE HS(FT) = 0.32   LARGEST HS(FT) = 1.05   ANGLE CLASS % = 8.6

STATION 1 20 YEARS ANGLE CLASS (DEG AZIMUTH) = 67.5
WATER DEPTH = 6.50 FEET
PERCENT OCCURRENCE(X1000) OF HEIGHT AND PERIOD BY DIRECTION

HEIGHT(FEET)	PERIOD(SECONDS)										TOTAL
	0.0-0.9	1.0-1.9	2.0-2.9	3.0-3.9	4.0-4.9	5.0-5.9	6.0-6.9	7.0-7.9	8.0-8.9	9.0-LONGER	
0. - 0.49	.	3880	1608	.	.	.	.	.	.	.	5488
0.50 - 0.99	.	.	626	.	.	.	.	.	.	.	626
1.00 - 1.49	.	.	.	3	.	.	.	.	.	.	3
1.50 - 1.99	.	.	.	.	.	.	.	.	.	.	0
2.00 - 2.49	.	.	.	.	.	.	.	.	.	.	0
2.50 - 2.99	.	.	.	.	.	.	.	.	.	.	0
3.00 - 3.49	.	.	.	.	.	.	.	.	.	.	0
3.50 - 3.99	.	.	.	.	.	.	.	.	.	.	0
4.00 - 4.49	.	.	.	.	.	.	.	.	.	.	0
4.50 - 4.99	.	.	.	.	.	.	.	.	.	.	0
5.00 - GREATER	.	.	.	.	.	.	.	.	.	.	0
TOTAL	0	3880	2234	3	0	0	0	0	0	0	

AVERAGE HS(FT) = 0.28   LARGEST HS(FT) = 1.21   ANGLE CLASS % = 6.1

Figure 17.   Sample percent occurrence tables for all seasons (20 years) by direction

WATER DEPTH = 6.50 FEET
PERCENT OCCURRENCE(X100) OF HEIGHT AND PERIOD FOR ALL DIRECTIONS

HEIGHT(FEET)	PERIOD(SECONDS)										TOTAL
	0.0-0.9	1.0-1.9	2.0-2.9	3.0-3.9	4.0-4.9	5.0-5.9	6.0-6.9	7.0-7.9	8.0-8.9	9.0-LONGER	
0. - 0.49	.	3267	3031	27	.	.	.	.	.	.	6325
0.50 - 0.99	.	.	2368	346	77	82	140	.	.	.	3013
1.00 - 1.49	.	.	7	182	48	.	58	.	.	.	295
1.50 - 1.99	.	.	.	1	39	.	.	.	.	.	40
2.00 - 2.49	.	.	.	.	2	.	.	82	.	.	84
2.50 - 2.99	.	.	.	.	.	.	.	10	24	5	39
3.00 - 3.49	.	.	.	.	.	.	.	.	.	3	3
3.50 - 3.99	.	.	.	.	.	.	.	.	.	.	0
4.00 - 4.49	.	.	.	.	.	.	.	.	.	.	0
4.50 - 4.99	.	.	.	.	.	.	.	.	.	.	0
5.00 - GREATER											0
TOTAL	0	3267	5406	556	166	82	198	92	24	8	

AVE HS(FT) = 0.45   LARGEST HS(FT) = 3.19   TOTAL CASES =   58440

Figure 18.   Sample percent occurrence table for all seasons
(20 years) and all directions

The following tabulation lists the approximate number of hours in each
season for 1 year:

Season	Number of Hours in Season for 1 Year
1 (D, J, F)	~2166
2 (M, A, M)	~2208
3 (J, J, A)	~2208
4 (S, O, N)	~2184

The total number of hours in the time interval for a specified season
can be found by multiplying the number of hours listed in the above
tabulation by the number of years required for a given problem.

62.   The all-directions tables can be used in a similar fashion.
To find the number of hours waves ≥ 1.0 ft and < 1.5 ft are expected to
occur within a year for Station 1 in Season 1 for all directions and
periods, divide the value in the total column for the specified H_s
range by 100, which yields a percent of 0.36 (Figure 16).   Divide 0.36
by 100 to get the probability; then multiply by the number of hours in
Season 1 for 1 year.   That is:

$$\frac{360}{100} \div 100 \times 2,166 \cong 78 \text{ hr}$$

63. This procedure may also be used when dealing with the data in the 20-year angle class and all-directions tables. The number of hours in the time interval found in Equation 25 would now be the sum for all four seasons or 8,766 hours per year.

Percent Exceedance Diagrams

Description

64. The percent exceedance diagrams (Figure 19) were constructed for all months in the 20 years of hindcast significant wave-height data. The diagrams have a log scale percent axis to allow greater accuracy for the larger wave-height categories. One must note that the larger wave-height categories will be affected by tropical storm conditions. The calculations performed in this study assumed all storm-generated winds and waves were derived from only extratropical conditions, even though tropical storm periods were included.

Example

65. To find the percent of time that a 3-ft wave is exceeded at Station 1, locate the 3-ft intersect with the curve supplied in the diagram (Figure 19) and read the percent exceeded from the percent axis (for this example, ~0.025 percent).

Height, Period, Direction Histograms

Description

66. Histograms for each station are presented for seasonal (Figure 20) and full 20-year data (Figure 21). The histograms show the percent occurrence of significant waves as a function of the three basic wave parameters (H_s, T, and ψ).

Use of the diagrams

67. These diagrams are intended for use as visual aids and relatively gross estimations.

Example

68. For the 20-year record of Station 1 wave conditions, approximately 30 percent of the waves were between 0.5 and 1.0 ft in
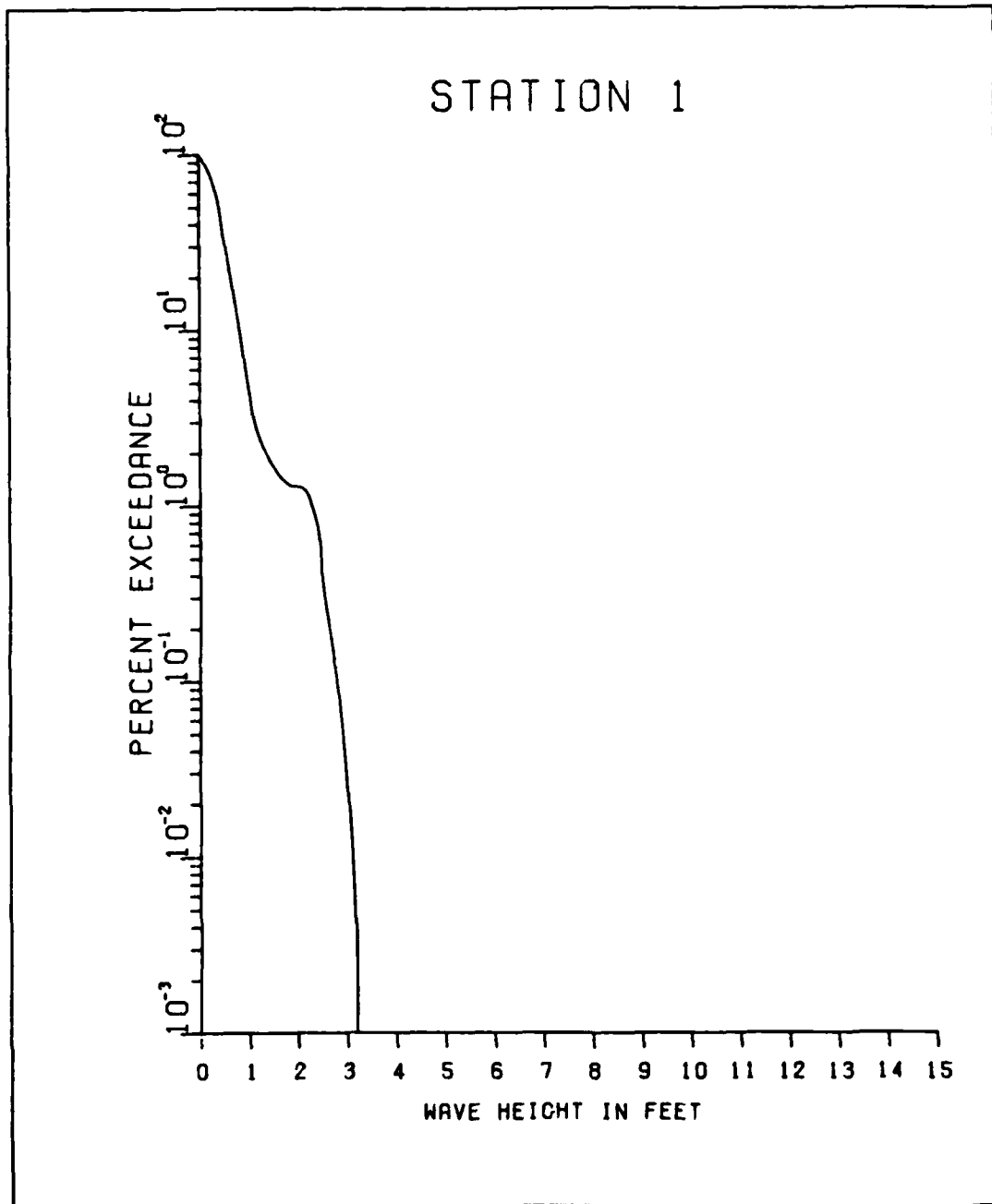
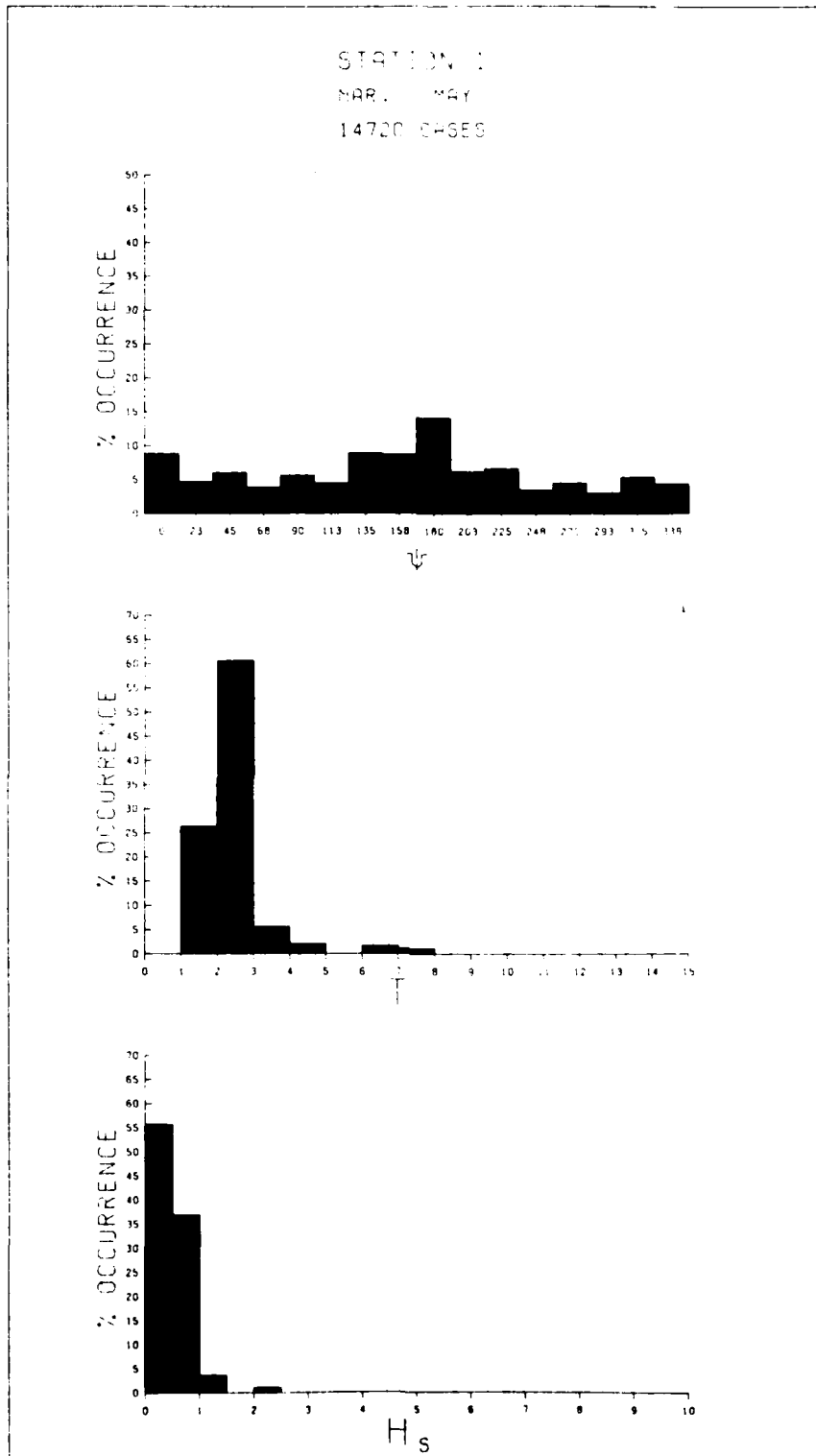Figure 19. Sample percent exceedance diagram

45

Figure 20.   Sample height, period, and direction
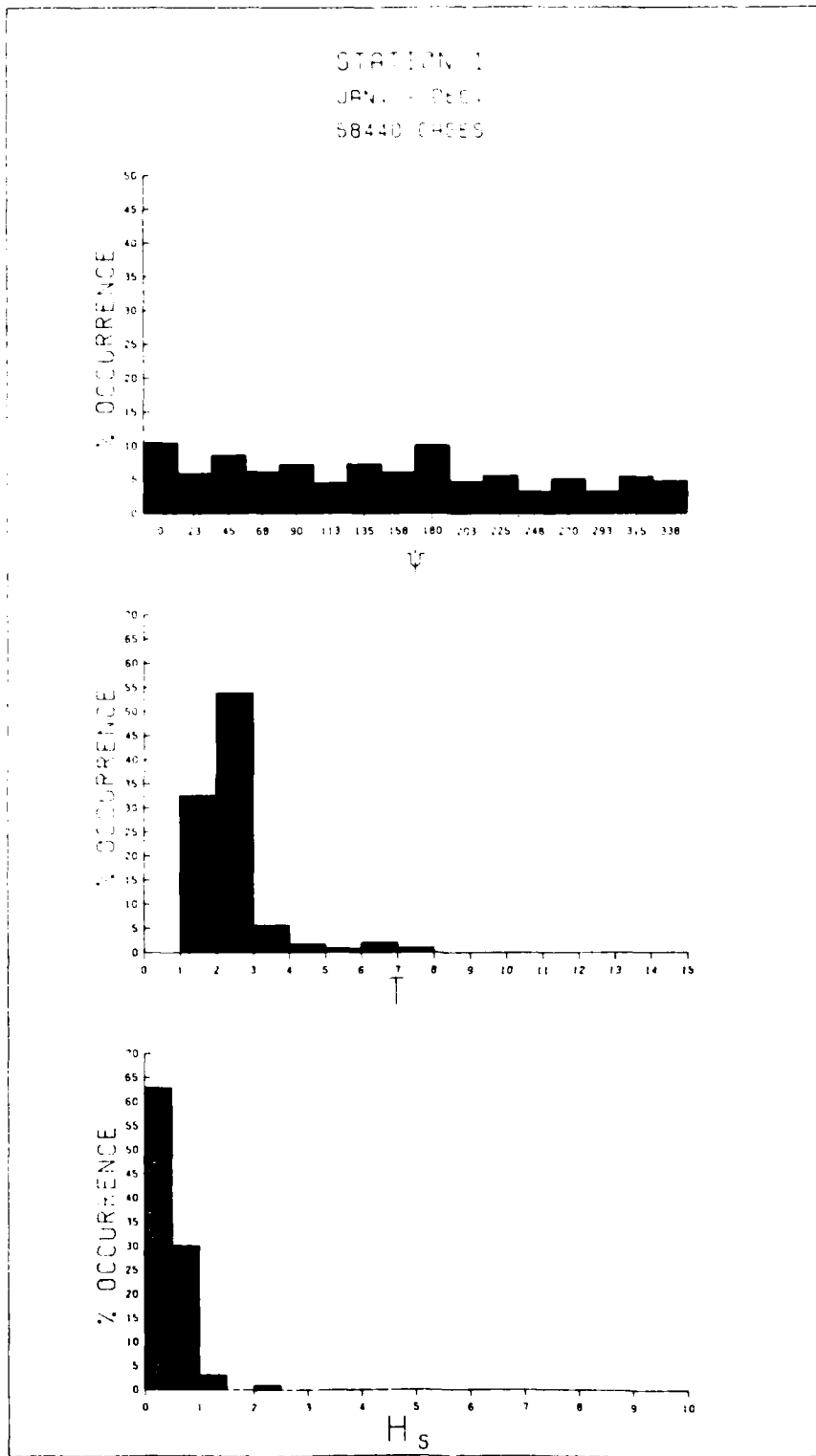histograms by season

Figure 21. Sample height, period, and direction
histograms for all seasons (20 years)

height (H_s) , about 6 percent of the waves had peak wave periods between 3.0 and 4.0 sec (T), and more waves came from 0-deg and 180-deg angle classes (ψ) than any other category (Figure 21).

Mean and Largest H_s Table

Description

69. Two tables which summarize the mean and largest H_s for each month and year are provided for each station (Figure 22). The mean table also provides a mean monthly value and a mean yearly value for H_s . The largest H_s table provides the largest H_s hindcast for each year and month as well as the largest H_s hindcast for the specified station.

Use of the tables

70. The tables can be used as a quick reference in determining gross estimates of the wave climate of an area. Due to extreme variations in wave heights, the mean H_s value is of little use beyond gross estimates. The largest H_s value provides an idea of what extreme significant wave heights might occur; however, other data products presented in this report can assist in determining how often to expect extreme values and how long they might occur.

Example

71. To determine the mean H_s at Station 1 for January 1956, simply read the value in the specified column and row (Figure 22). The mean H_s for 1956 is given in the mean column opposite 1956. The mean H_s for all January's is given in the mean row under January for this example:

    a. The mean H_s for January 1956 = 0.5 ft.

    b. The mean H_s for 1956 = 0.4 ft.

    c. The mean H_s for all January's = 0.5 ft

The largest H_s table can be read in a similar fashion, and by scanning the columns and rows, additional information can be determined (Figure 22).

    a. The largest H_s for January 1956 = 2.5 ft.

    b. The largest H_s for 1956 = 2.6 ft.

    c. The largest H_s for all January's = 3.2 ft.

MEAN HS(FEET) BY MONTH AND YEAR

STATION   1

MONTH

YEAR	JAN	FEB	MAR	APR	MAY	JUN	JUL	AUG	SEP	OCT	NOV	DEC	MEAN
1956	0.5	0.4	0.4	0.4	0.3	0.4	0.4	0.3	0.3	0.3	0.4	0.4	0.4
1957	0.4	0.4	0.4	0.4	0.4	0.3	0.4	0.4	0.3	0.4	0.5	0.4	0.4
1958	0.5	0.5	0.5	0.6	0.4	0.4	0.4	0.4	0.4	0.5	0.5	0.6	0.5
1959	0.5	0.5	0.6	0.5	0.4	0.5	0.4	0.5	0.5	0.5	0.6	0.6	0.5
1960	0.6	0.7	0.7	0.5	0.5	0.4	0.5	0.3	0.4	0.4	0.5	0.5	0.5
1961	0.6	0.7	0.6	0.7	0.5	0.4	0.4	0.4	0.4	0.5	0.6	0.6	0.5
1962	0.7	0.7	0.7	0.5	0.5	0.4	0.4	0.3	0.3	0.3	0.4	0.4	0.5
1963	0.4	0.5	0.4	0.5	0.5	0.5	0.4	0.4	0.4	0.3	0.5	0.6	0.5
1964	0.6	0.7	0.6	0.6	0.4	0.4	0.5	0.4	0.4	0.6	0.5	0.6	0.5
1965	0.6	0.7	0.7	0.6	0.5	0.5	0.4	0.4	0.4	0.5	0.4	0.4	0.5
1966	0.5	0.6	0.6	0.7	0.5	0.4	0.4	0.3	0.3	0.3	0.4	0.5	0.5
1967	0.4	0.5	0.5	0.5	0.5	0.4	0.5	0.3	0.3	0.4	0.5	0.5	0.4
1968	0.4	0.5	0.5	0.4	0.4	0.4	0.3	0.4	0.3	0.3	0.5	0.5	0.4
1969	0.5	0.5	0.6	0.5	0.4	0.4	0.4	0.3	0.3	0.4	0.4	0.5	0.4
1970	0.4	0.5	0.5	0.5	0.4	0.5	0.4	0.4	0.4	0.5	0.6	0.6	0.5
1971	0.4	0.6	0.7	0.6	0.5	0.6	0.5	0.5	0.3	0.3	0.4	0.4	0.5
1972	0.5	0.4	0.5	0.5	0.4	0.6	0.4	0.4	0.3	0.4	0.5	0.4	0.4
1973	0.5	0.5	0.5	0.6	0.6	0.4	0.3	0.3	0.4	0.3	0.4	0.6	0.5
1974	0.4	0.5	0.5	0.5	0.5	0.4	0.4	0.3	0.4	0.3	0.4	0.5	0.4
1975	0.4	0.5	0.5	0.4	0.3	0.4	0.4	0.3	0.3	0.3	0.4	0.4	0.4
MEAN	0.5	0.6	0.6	0.5	0.5	0.4	0.4	0.4	0.4	0.4	0.5	0.5	

LARGEST HS(FEET) BY MONTH AND YEAR

STATION   1

MONTH

YEAR	JAN	FEB	MAR	APR	MAY	JUN	JUL	AUG	SEP	OCT	NOV	DEC
1956	2.5	2.4	2.5	2.4	1.1	1.1	2.5	1.0	1.2	1.1	1.4	2.6
1957	2.4	2.4	2.7	2.8	2.4	1.2	2.4	2.3	1.0	1.0	2.4	2.6
1958	2.8	2.8	2.6	2.8	2.4	2.5	2.7	2.3	1.0	2.4	1.7	2.3
1959	2.5	2.3	2.6	1.2	1.5	2.5	1.1	2.5	2.4	2.9	2.4	2.9
1960	3.2	2.8	3.1	2.9	2.4	2.8	2.4	2.3	1.8	1.4	1.2	2.9
1961	3.1	2.9	2.9	3.1	2.6	2.3	2.4	2.3	1.3	2.4	2.9	2.7
1962	3.0	2.7	3.0	2.2	2.3	2.6	2.3	1.2	1.2	1.0	2.4	2.4
1963	1.7	2.5	2.6	2.5	2.6	2.3	2.4	2.3	1.5	1.0	3.0	2.3
1964	3.0	3.2	3.0	2.4	2.3	2.5	2.7	2.4	1.0	2.3	2.4	2.5
1965	3.0	3.0	2.9	2.7	2.6	2.6	2.7	2.8	1.2	2.4	2.6	1.1
1966	2.6	2.9	2.8	3.0	1.2	1.3	2.3	1.4	1.4	2.3	1.5	2.7
1967	2.4	2.4	2.5	2.7	2.4	2.3	2.4	1.3	1.2	1.3	2.3	2.9
1968	2.9	2.3	2.8	2.3	2.5	2.5	1.1	2.6	1.0	1.1	2.5	2.7
1969	2.3	2.4	2.9	2.8	2.3	2.3	2.3	2.4	1.2	2.3	2.4	2.7
1970	2.3	2.5	2.7	2.3	1.2	2.7	2.8	2.5	2.3	2.4	2.7	2.7
1971	2.7	2.9	3.0	2.8	2.7	2.3	2.3	2.7	1.3	2.3	2.4	1.1
1972	2.4	2.6	2.9	2.3	1.2	2.7	2.4	2.4	2.5	2.3	2.6	2.6
1973	2.5	2.6	2.7	2.6	2.5	2.4	1.2	2.3	1.4	1.6	2.8	2.8
1974	2.4	2.6	2.5	2.3	2.4	2.3	2.5	1.2	1.2	0.8	2.6	2.6
1975	2.3	2.5	2.3	1.2	1.1	2.6	1.4	2.4	1.5	1.4	1.4	2.7

LARGEST HS(FEET) FOR STATION   1 =   3.2

Figure 22.   Sample mean   H$_s$ and largest   H$_s$ tables

49

Duration Tables

Description

72. These tables contain H_s duration information for all 23 Mississippi Sound stations. The values given in the tables are the mean duration in hours $(\bar{x})$ and the maximum duration in hours (mx). For the "over" tables (Figure 23 and Appendix F), duration is defined as the length of time waves greater than a given height persist once the wave height has been exceeded, and for the "under" tables (Figure 24 and Appendix G), duration is the length of time waves less than a given height persist once the waves become less than the indicated H_s category. The computations used data from all months of the 20-year hindcast wave data.

Use of the tables

73. For sequences of wave heights, discretized sets of durations are formed of wave heights above or below a specified level after waves exceed or become less than that level. Each element of an individual *set is a single duration event, and the expected* duration above or below a specified level is equal to the mean of all elements in the set. Thus:

$$\bar{x}_j = \sum_{i=1}^{n_j} x_{ij}$$

where

      subscript j = an incremented wave-height counter for wave height h_j

               i = a counter for duration events

              n = number of times that waves exceed or become less than a particular wave height

          x_{ij} = duration of a single event with wave heights above or below level H_j

In this formulation a number of other useful duration parameters from the 20-year sample can be estimated.

Duration of Waves over a Specified Height

Wave Height Class ft	Station 1 x̄	mx	Station 2 x̄	mx	Station 3 x̄	mx	Station 4 x̄	mx	Station 5 x̄	mx	Station 6 x̄	mx	Station 7 x̄	mx	Station 8 x̄	mx
>0.5	9	117	14	261	14	198	14	261	16	273	14	249	12	174	9	150
>1.0	5	30	6	54	7	81	7	90	7	114	7	114	6	93	6	78
>1.5	4	18	5	30	5	39	6	45	5	42	5	57	5	42	5	27
>2.0	4	15	4	15	4	18	4	21	4	18	4	18	4	18	4	15
>2.5	4	15	4	15	4	6	4	18	4	15	4	15	4	15	3	9
>3.0	3	6	4	15	3	3	4	15	4	15	4	15	4	15	3	3
>3.5	--	--	4	15	--	--	4	15	4	15	4	15	4	15	--	--
>4.0	--	--	4	12	--	--	4	15	4	15	4	15	3	6	--	--
>4.5	--	--	3	3	--	--	4	12	4	9	4	15	--	--	--	--
>5.0	--	--	--	--	--	--	3	6	3	3	3	3	--	--	--	--
>5.5	--	--	--	--	--	--	3	3	--	--	--	--	--	--	--	--
>6.0	--	--	--	--	--	--	--	--	--	--	--	--	--	--	--	--
>6.5	--	--	--	--	--	--	--	--	--	--	--	--	--	--	--	--
>7.0	--	--	--	--	--	--	--	--	--	--	--	--	--	--	--	--

(continued)

Note: x̄ equals the mean duration in hours for the specified wave-height class; mx equals the maximum duration in hours for the specified wave-height class.

Figure 23. Sample "over" duration table

Duration of Waves Under a Specified Height

Wave Height Class ft	Station 1 x̄	mx	Station 2 x̄	mx	Station 3 x̄	mx	Station 4 x̄	mx	Station 5 x̄	mx
Calm	3	3	3	3	3	3	3	6	3	3
<0.5	19	273	12	135	11	165	11	180	9	96
<1.0	105	1,365	53	804	37	804	37	633	24	492
<1.5	246	3,447	185	2,727	165	3,111	121	2,277	91	981
<2.0	299	3,447	273	3,099	932	8,682	236	2,727	186	2,244
<2.5	1,113	6,969	293	3,111	6,649	40,185	280	3,111	212	3,084
<3.0	8,178	35,484	294	3,111	53,218	114,498	293	3,111	214	3,084
<3.5	--	--	843	6,213	--	--	414	6,165	577	6,165
<4.0	--	--	2,809	14,721	--	--	1,157	8,241	1,619	17,369
<4.5	--	--	11,828	35,484	--	--	2,809	14,721	3,639	33,180
<5.0	--	--	--	--	--	--	7,384	42,978	11,828	35,484
<5.5	--	--	--	--	--	--	35,490	35,742	--	--
<6.0	--	--	--	--	--	--	--	--	--	--
<6.5	--	--	--	--	--	--	--	--	--	--
<7.0	--	--	--	--	--	--	--	--	--	--

(continued)

Note: x̄ equals the mean duration in hours for the specified wave-height class; mx equals the maximum duration in hours for the specified wave-height class.

Figure 24. Sample "under" duration table

51

<u>a</u>. x_{jmax} - the maximum duration of waves above or below H_j .

<u>b</u>. x_{jmin} - the minimum duration of waves greater than or less than H_j .*

<u>c</u>. $p(x_j)$ - the probability of occurrence of a particular duration of wave heights greater than or less than H_j .

<u>d</u>. $F(x_j)$ - the cumulative probability of occurrence of durations less than or greater than x for a particular H_j category.

<u>e</u>. $F'(x_j)$ - the cumulative probability that a duration event in category H_j will exceed or be less than length x .

74. In particular, the parameter $F'(x_j)$ plays a significant role in the assessment of design criteria when such criteria are based on expected damage as a function of duration of given wave conditions. For example, if the wave height associated with a 20-year return period has an expected duration of 3 hr, and it takes a 6-hr duration to significantly damage a structure, it becomes relevant to determine the probability of a 6-hr (or greater) duration at this wave height. In this sense, the design wave height would become a function of both wave height and duration, and optimization of design would require the consideration of both $F(x_j)$ and $F'(x_j)$.

<u>Example</u>

75. To find the mean and maximum duration for waves greater than 2.0 ft and less than 2.5 ft for Station 1, look up Station 1 in the "over" duration table and read the values in the >2.0 ft row. For this example, 4 hr is the mean and 15 hr is the maximum (Figure 23).

---

* Since this is calculated only when H_j is exceeded, this number is not zero; however, for most intermediate to high wave heights, the value of x_{jmin} is equal to the duration associated with one sample. Only for small waves does this parameter have significance.

PART V: DISCUSSION OF RESULTS

76.   This report presents the three major phases of the Mississippi
Sound Wave-Hindcast Study:

> a. Estimation of long-term wind conditions overwater.
>
> b. Development of a parametric shallow-water wave model.
>
> c. Calculation of long-term wave statistics for the study
>   area.

Each phase of the study was treated in detail, since errors in any phase
could alter the results in subsequent phases dramatically.   The estima-
tion of wind conditions in Mississippi Sound from overland wind condi-
tions employed techniques that have been verified through extensive
field studies (Resio and Vincent 1976).   The only assumption affecting
the wind results was: for each time interval, wind speeds and direc-
tions were uniform over the Sound.   This assumption was verified in
PART II of this report.

77.   The basis for the development of the Shallow-Water Wave Model
(SWWM) was to adequately describe the physical process involved in wave
growth and finite depth wave transformations while maximizing computa-
tional efficiency.   Detailed comparisons of the SWWM results with mea-
sured and visual observations in Mississippi Sound are necessary for
verification.   Unfortunately, only limited wave data were available in
Mississippi Sound to perform comparisons; and verification of the mod-
eling technique is not possible with such limited information.   Results
from another study employing the SWWM (Appendix A and Garcia and Jensen,
in preparation) were presented and clearly showed that the hindcast data
compare favorably with the measured wave data.   The physical processes
and geometry associated with both studies are very similar (excluding
tropical storms).   Therefore, it is reasonable to assume the SWWM ade-
quately models finite water depth wave growth and transformation pro-
cesses and that application to Mississippi Sound is valid.

REFERENCES

Barnett, T. P.   1968.   "On the Generation, Dissipation and Prediction of Ocean Wind Waves," Journal of Geophysical Research, Vol 73, pp 513-529.

Bretschneider, C. L.   1952.   "The Generation and Decay of Wind Waves in Deep Water," Transactions, American Geophysical Union, Vol 33, No. 3, pp 381-389.

_____.   1954.   "Generation of Wind Waves over a Shallow Bottom," Technical Memorandum No. 51, Beach Erosion Board, CE.

Bretschneider, C. L., and Reid, R. 0.   1954.   "Changes in Wave Height due to Bottom Friction, Percolation and Refraction," Technical Memorandum No. 45, Beach Erosion Board, CE.

Cavalri, L., and Rizzoli, P. M.   1981.   "Wind Wave Prediction in Shallow Water: Theory and Application," Journal of Geophysical Research, Vol 86, No. C11, pp 10,961-10,973.

Collins, I. A.   1972.   "Prediction of Shallow Water Wave Spectra," Journal of Geophysical Research, Vol 17, No. 15, pp 2693-2707.

Garcia, A. W., and Jensen, R. E.   "Wave Data Acquisition and Hindcast for Saginaw Bay" (in preparation), U. S. Army Engineer Waterways Experiment Station, CE, Vicksburg, Miss.

Goda, Y.   1974.   "Estimation of Wave Statistics from Spectral Information," Proceedings, International Symposium on Ocean Wave Measurement and Analysis, American Society of Civil Engineers, Vol 1, pp 320-337.

Hasselmann, K.   1962.   "On the Non-Linear Energy Transfer in a Gravity Wave Spectrum-General Theory," Journal of Fluid Mechanics, Vol 12, Part 1, pp 481-500.

Hasselmann, K., et al.   1973.   "Measurements of Wind-Wave Growth and Swell Decay During the Joint North Sea Wave Project JONSWAP," Dtsch, Hydrogr. Z., Vol 8, Supplement A8, No. 12.

_____.   1976.   "A Parametric Wave Prediction Model," Journal of Physical Oceanography, Vol 6, pp 200-228.

Heterich, K., and Hasselmann, K.   1980.   "A Similarity Relation for the Non-Linear Energy Transfers in a Finite-Depth Gravity-Wave Spectrum," Journal of Fluid Mechanics, Vol 97, Part 1, pp 215-224.

Hsiao, Shu-Chi V.   1978.   "On the Transformation Mechanisms and the Prediction of Finite-Depth Water Waves," Ph. D. Dissertation, University of Florida, Gainesville, Fla.

Iwata, K.   1980.   "Wave Spectrum Changes due to Shoaling and Breaking; I - Minus - Three - Power - Law on Frequency Spectrum," Osaka University, Technical Report, Vol 30, No. 1517-1550, pp 269-278.

Jensen, R. E.   "Methodology for the Calculation of a Shallow-Water Wave Climate," WIS Report 8 (in preparation), U. S. Army Engineer Waterways Experiment Station, CE, Vicksburg, Miss.

Johnson, J. W., O'Brien, M. P., and Isaacs, J. D. 1948. "Graphical Construction of Wave Refraction Diagrams," HO No. 605, TR-2, U. S. Naval Oceanographic Office, Washington, D. C.

Kitaigordskii, S. A. 1962. "Application of the Theory of Similarity to the Analysis of Wind-Generated Wave Motion as a Stochastic Process," Bull. Acad. Sci. USSR Ser. Geophys., Vol 1, No. 1, pp 105-117.

Kitaigordskii, S. A., Krasitskii, V. P., and Zaslavaskii, M. M. 1975 (Jul). "On Phillips' Theory of Equilibrium Range in the Spectra of Wind-Generated Gravity Waves," Journal of Physical Oceanography, Vol 5, No. 3, pp 410-420.

Mitsuyasu, H. 1968. "On the Growth of the Spectrum of Wind-Generated Waves (I)," Reports of Research Institute for Applied Mechanics, Kyushu University, Vol 16, No. 55, pp 459-482.

_____. 1969. "On the Growth of the Spectrum of Wind-Generated Waves (II)," Reports of Research Institute for Applied Mechanics, Kyushu University, Vol 17, No. 59, pp 235-248.

Mitsuyasu, H., and Kimura, H. 1965. "Wind Wave in Decay Area," Coastal Engineering in Japan, Vol 8, pp 21-35.

Neumann, C. J., et al. 1978. "Tropical Cyclones of the North Atlantic Ocean, 1871-1977," National Climatic Center, Asheville, N. C., and the National Hurricane Center, Coral Gables, Fla.

Ou, Shan-Hwei. 1980 (Sep). "The Equilibrium Range in the Frequency Spectra of the Wind Generated Gravity Waves," Proceedings, 4th Conference on Ocean Engineering in the Republic of China.

Phillips, O. M. 1957. "On the Generation of Waves by Turbulent Wind," Journal of Fluid Mechanics, Vol 2, pp 417-445.

_____. 1958. "The Equilibrium Range in the Spectrum of Wind Generated Waves," Journal of Fluid Mechanics, Vol 4, pp 426-434.

Resio, D. T., and Vincent, C. L. 1976 (Jun). "Estimation of Winds over the Great Lakes," Miscellaneous Paper H-76-12, U. S. Army Engineer Waterways Experiment Station, CE, Vicksburg, Miss.

Shemdin, O. H., et al. 1980. "Mechanisms of Wave Transformation in Finite-Depth Water," Journal of Geophysical Research, Vol 85, No. C9, pp 5012-5018.

Thornton, E. B. 1977. "Rederivation of the Saturation Range in a Frequency Spectrum of Wind-Generated Gravity Waves," Journal of Physical Oceanography, Vol 7, pp 137-140.

U. S. Army Coastal Engineering Research Center, CE. 1977. "Shore Protection Manual," 3rd ed. (Vols I, II, and III), Stock No. 008-022-00113-1, U. S. Government Printing Office, Washington, D. C.

_____. 1981. "Method of Determining Adjusted Windspeed, U_A, for Wave Forecasting," CETN-I-5, Fort Belvoir, Va.

U. S. Army Coastal Engineering Research Center, CE. 1981. "Revised Method for Wave Forecasting in Shallow Water," CETN-I-6, Fort Belvoir, Va.

U. S. Army Engineer District, Mobile. 1981. "Mississippi Sound Data Collection Program Draft Final Report," Contract No. DACW01-80-6-0104, Prepared by Raytheon Ocean Systems Company, Portsmouth, R. I.

Vincent, C. L. 1981. "A Method for Estimating Depth-Limited Wave Energy," Rep. CETA 81-16, U. S. Army Coastal Engineering Research Center, CE, Fort Belvoir, Va.

_____. 1982 (May). "Shallow Water Wave Modeling," 1st International Conference on Meteorology and Air-Sea Interaction in the Coastal Zone, Hague.

Vincent, C. L., and Lichy, D. E. 1981. "ARSLOE Wave Measurements," Proceedings, Conference on Directional Wave Spectra Applications, American Society of Civil Engineers, pp 71-86.

APPENDIX A: VERIFICATION OF THE SHALLOW-WATER WAVE MODEL

1. The shallow-water wave model (SWWM) was first applied to a project in Saginaw Bay, Michigan, because wave data were already available for calibration and verification in that location. The bathymetry (except for navigational channels) and basin configuration of Mississippi Sound are somewhat similar to that in Saginaw Bay (Figure A1). Both basins are virtually cut off from adjacent expansive deepwater areas by shoals and islands. The assumptions and processes involved in the SWWM were the same for both the Saginaw Bay and Mississippi Sound studies. Four storm conditions were selected from the Saginaw Bay study to show the relative accuracy of the modeling technique. The scarcity of wave measurements in the Mississippi Sound region have resulted in the use of data from Saginaw Bay (having physical and geographical structures similar to the Sound) to verify the SWWM. Although th's is an indirect verification of the model for its use on Mississippi Sound, it is the only procedure available to provide a reasonable assurance that the model is valid for this application.

2. Measured wave and wind data from the 9-11 May 1981 storm were used to evaluate and verify the modeling technique in Saginaw Bay. The Corps anemometer was located approximately 12 miles southwest of Station 1. This storm (Figure A2) produced the largest waves recorded since initiation of that measurement program. These data were used to calibrate the SWWM within Saginaw Bay. A set of fetch lengths and water depths dependent on discrete wind direction angles were computed for each station (see Figure A1 for the station locations). The methodology used in the wave model was the same for both stations. Comparisons between the computed and measured H_s (significant wave height defined in Equation 21) at Stations 1 and 2 are shown in Figures A3 and A4. Comparisons between the computed and measured T (peak period, defined in Equation 22), are shown in Figures A5 and A6. The SWWM results compare very favorably with the measured H_s data for both stations; and the T results, over an average, also compare favorably with the measured data. One limitation to the SWWM is that it assumes discrete frequency bands

A1

of greater width than the results obtained by the analysis of the gage records. Large variations in the peak period are a function of time and cannot be resolved given near-constant wind conditions.

3. Three additional comparisons are performed and shown in Figures A7-A13. The first comparison BCT 1 (Blind Comparison Test) required a secondary source of wind data because the anemometer deployed near Saginaw Bay was not operable during the outline test period (5 and 6 May 1981). The secondary anemometer was at Wurtsmith Air Force Base located near Oscoda, Michigan (approximately 55 miles northeast of Station 1). The average wind condition for BCT 1 is approximately 15 mph, with maximum winds of 25 mph (Figure A7). The wind direction is shown to be highly variable during this particular storm (Figure A7). The results displayed in Figures A8 (H_s) and A9 (T) show how capable the SWWM is in computing accurate wave conditions under variable wind conditions. The next set of comparisons (BCT 2), for low wind speed conditions and variable wind directions (Figure A10), shows that the SWWM will predict the largest recorded H_s (~2.5 ft) in the event and approximate the associated T (~4.0 sec, Figure A11). There is an apparent divergence in the two data sets after the maximum condition is attained, but the differences are, at its maximum, 1.0 ft for H_s and 0.6 sec for T . The variability in the wind direction under low wind speeds could cause these differences. The last set of comparisons BCT 3 (Figures A12 and A13) is for near-constant wind directions and moderate wind speeds. Figure A12 displays two sets of wind information, the Corps anemometer (located near Bay City, approximately 10 miles southwest of Station 1) and Wurtsmith Air Force Base. One can see a major phase difference in the two data sets of approximately 14 hr. Using the Corps anemometer results for wind condition data in the model, we find that the hindcast wave results (Figure A13) for both H_s and T lag the measured results by the same 14 hr. The storm event is correctly simulated by the SWWM, where maximum differences fall within ±0.5 ft for H_s and ±0.5 sec for T , if the hindcast data are shifted 14 hr.

4. The data presented in this discussion are only examples of many comparisons made between measured and hindcast results. The only

A2

changes made in these comparisons were the input wind conditions.   No
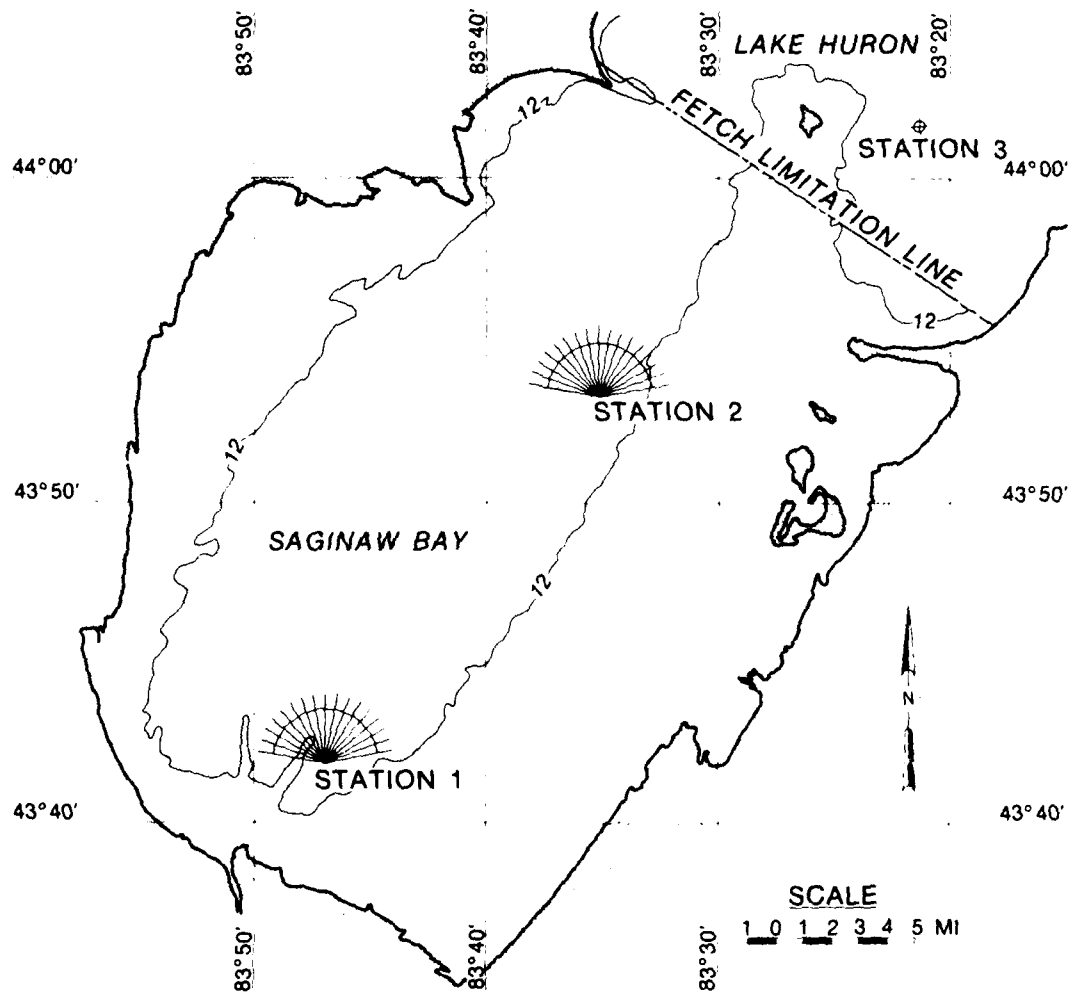adjustments in coefficients or mechanisms were made in the SWWM.
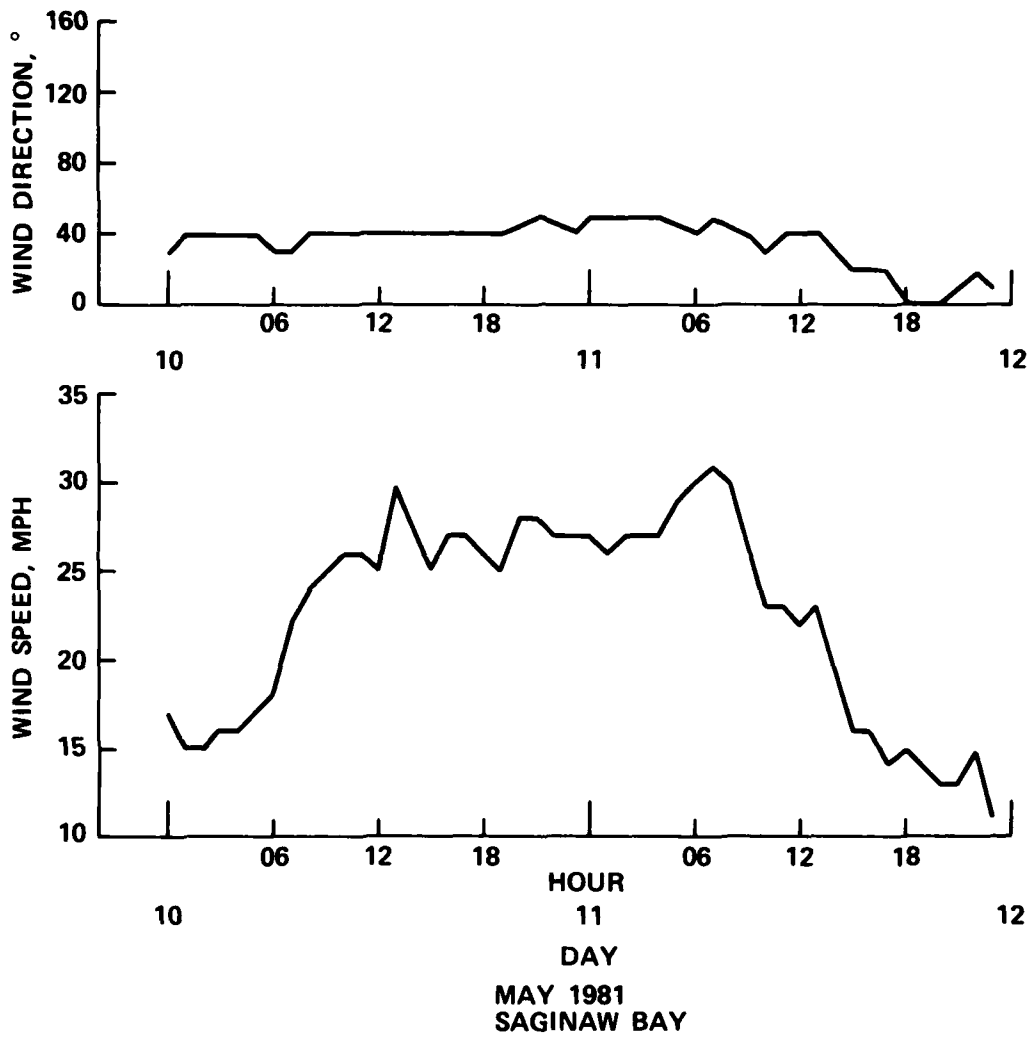
Figure A1.   Saginaw Bay station locations

A4

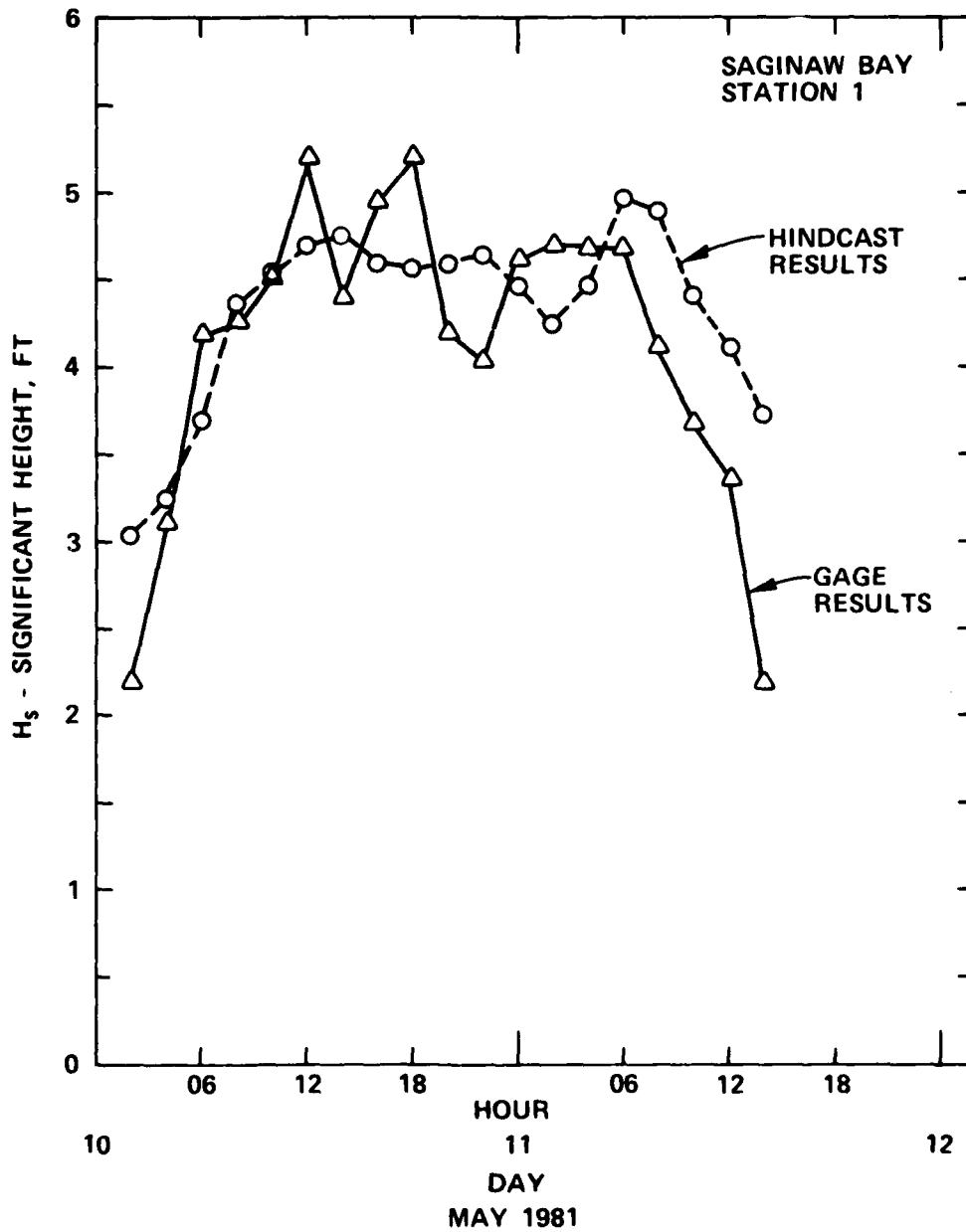Figure A2. Wind information for calibration test

A5

Figure A3.   Comparison between measured and hindcast significant
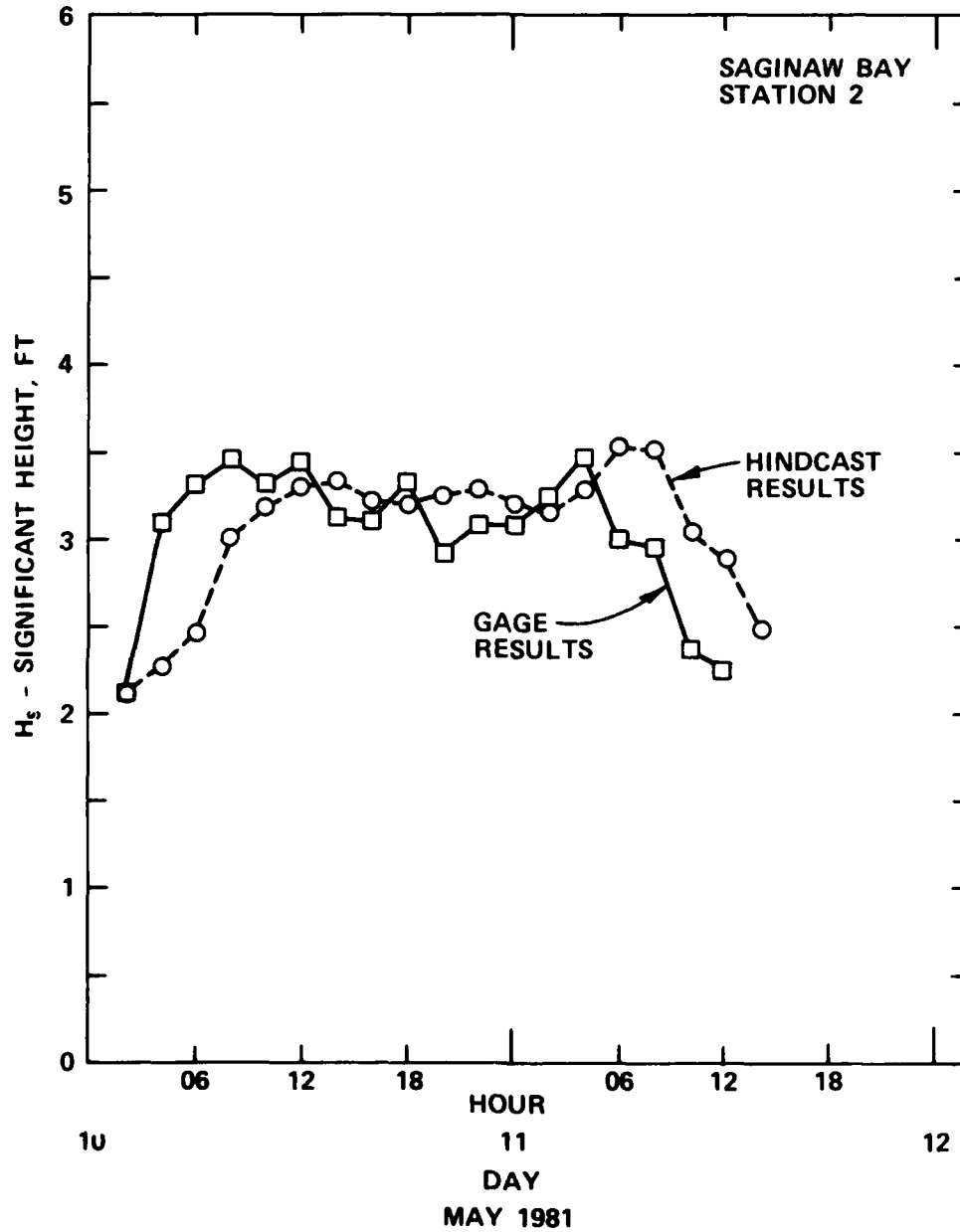wave-height data for Station 1

Figure A4. Comparison between measured and hindcast significant
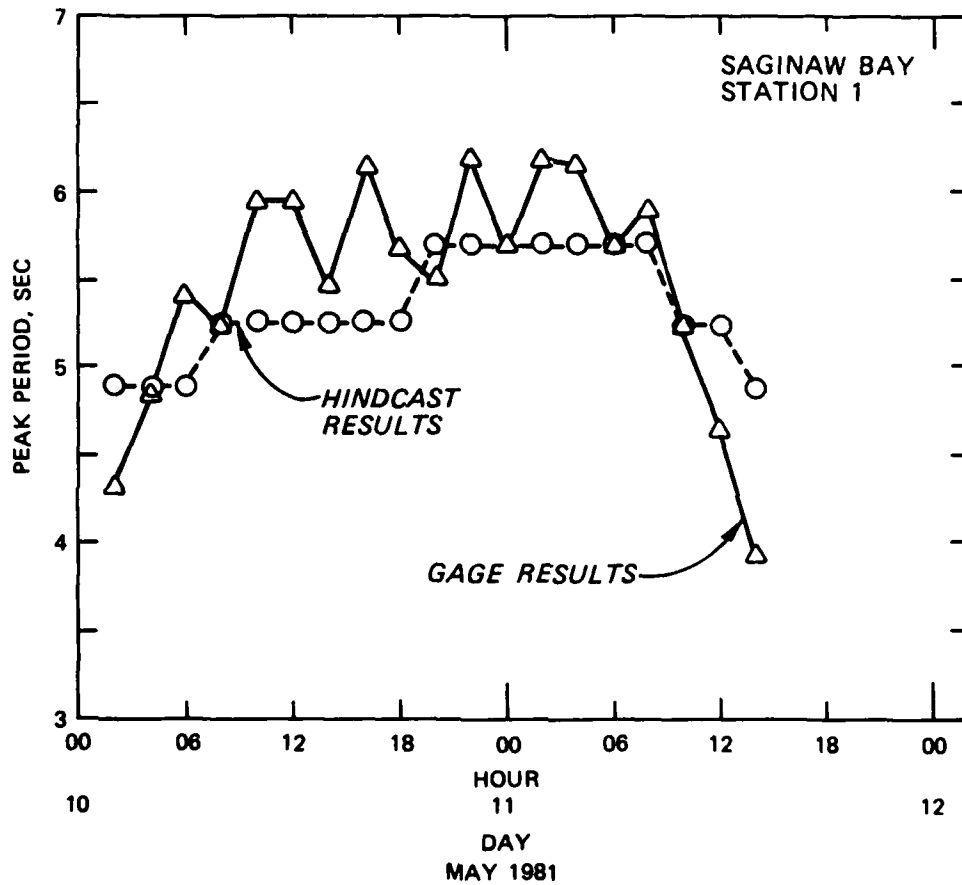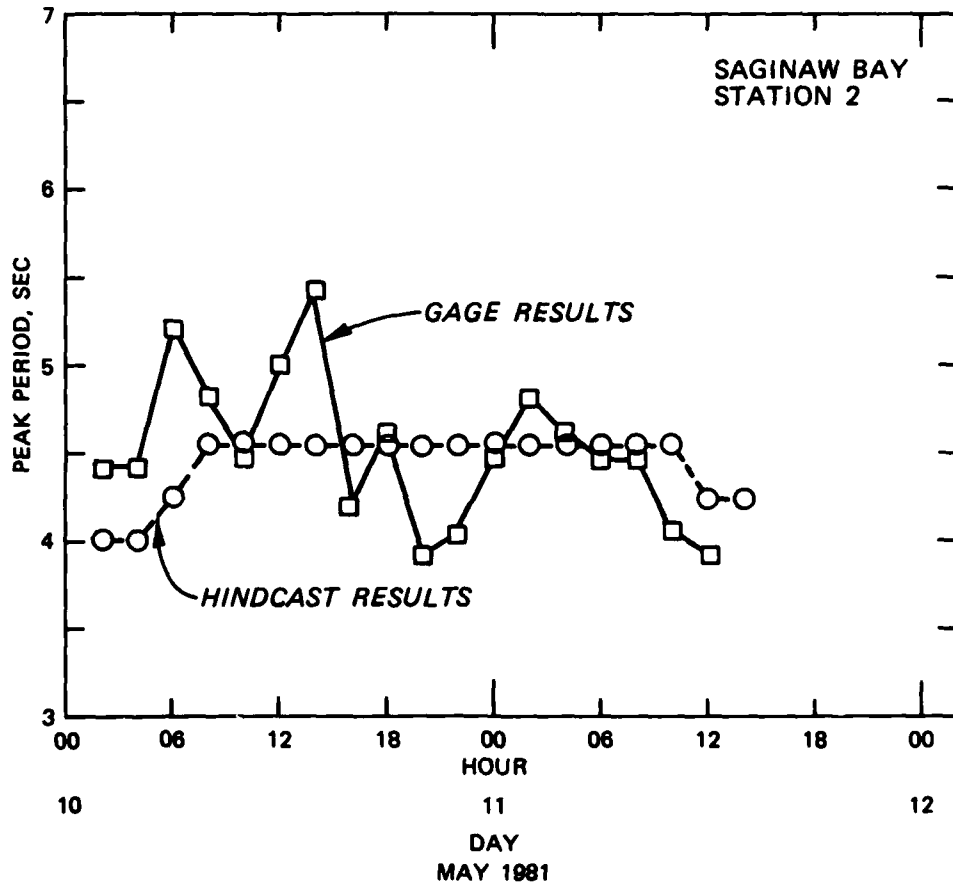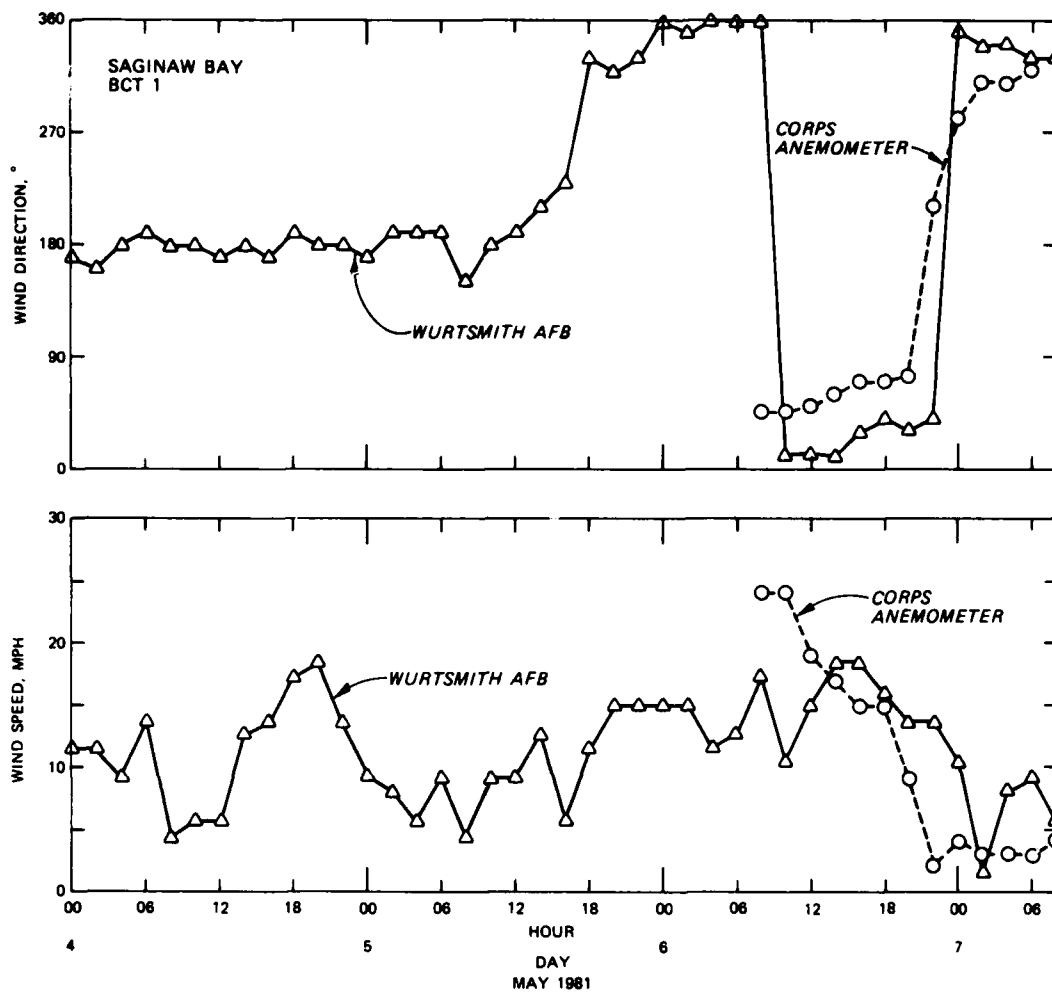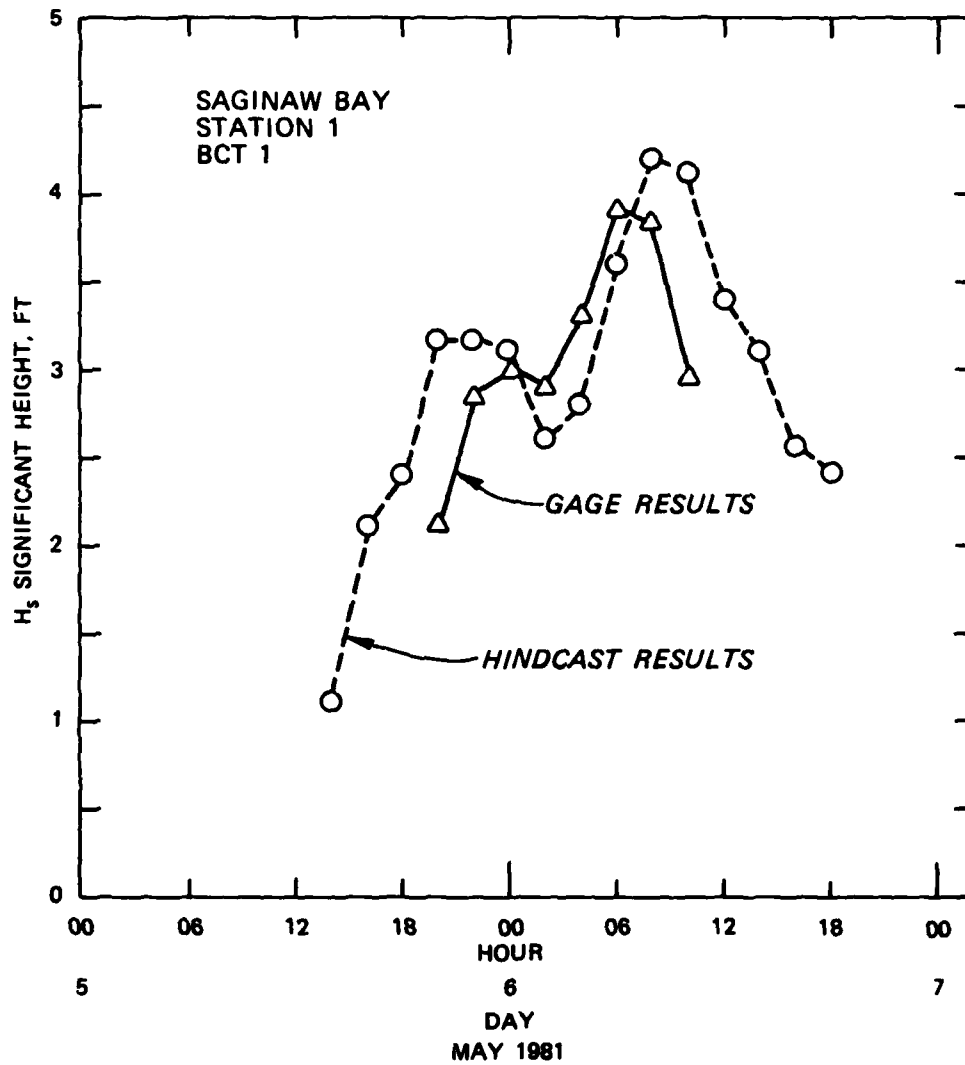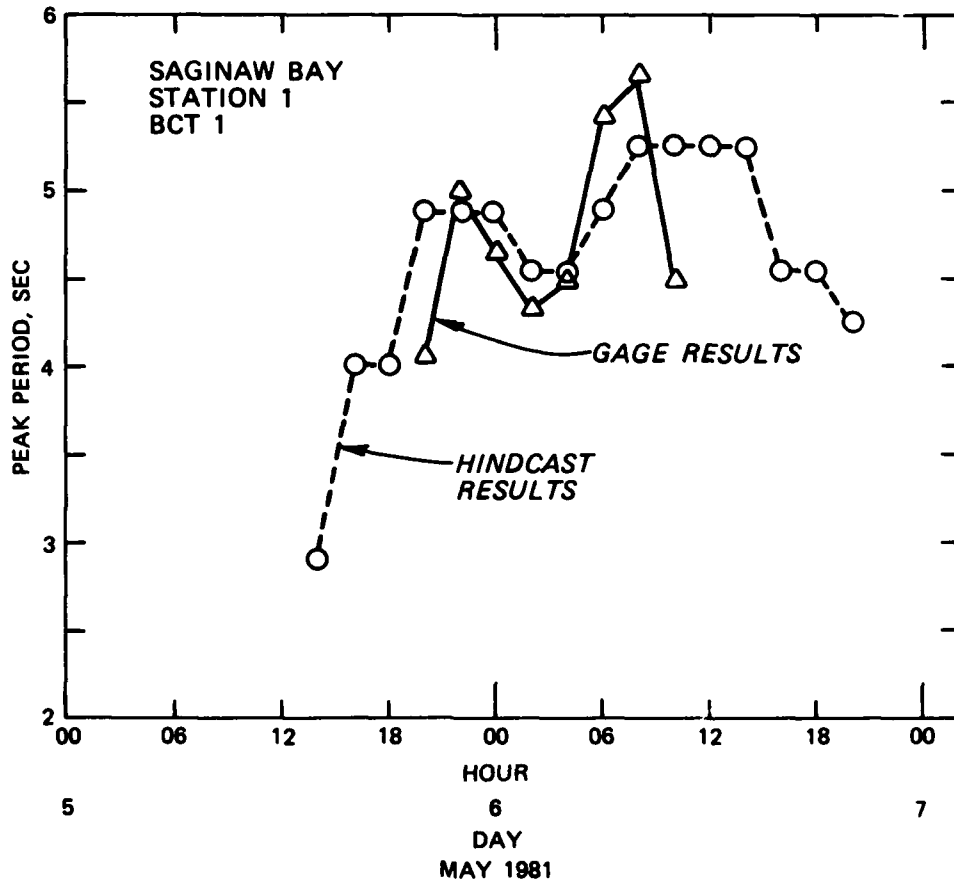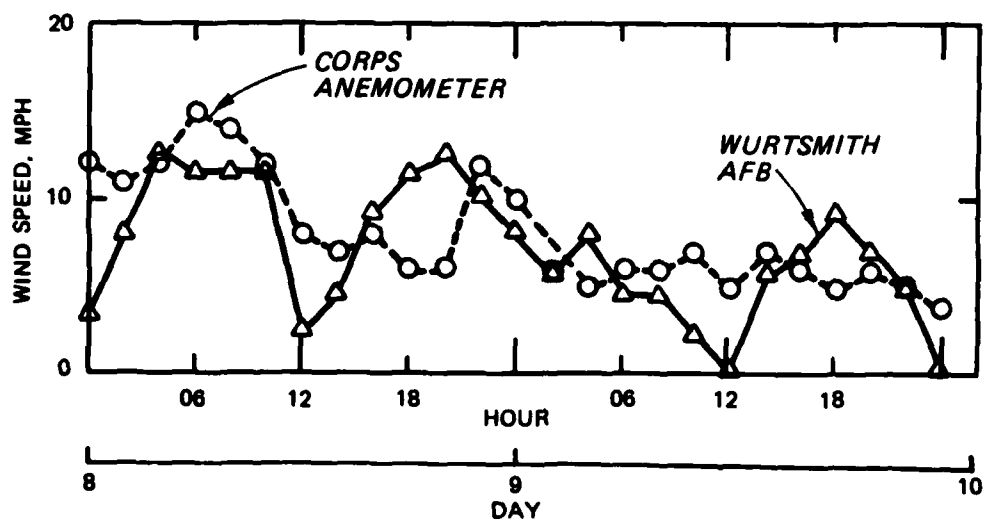wave-height data for Station 2

Figure A5. Comparison between measured and hindcast peak wave period data for Station 1

Figure A6. Comparison between measured and hindcast peak wave
period data for Station 2

Figure A7. Wind information data for BCT 1

A10

Figure A8. Comparison between measured and hindcast significant
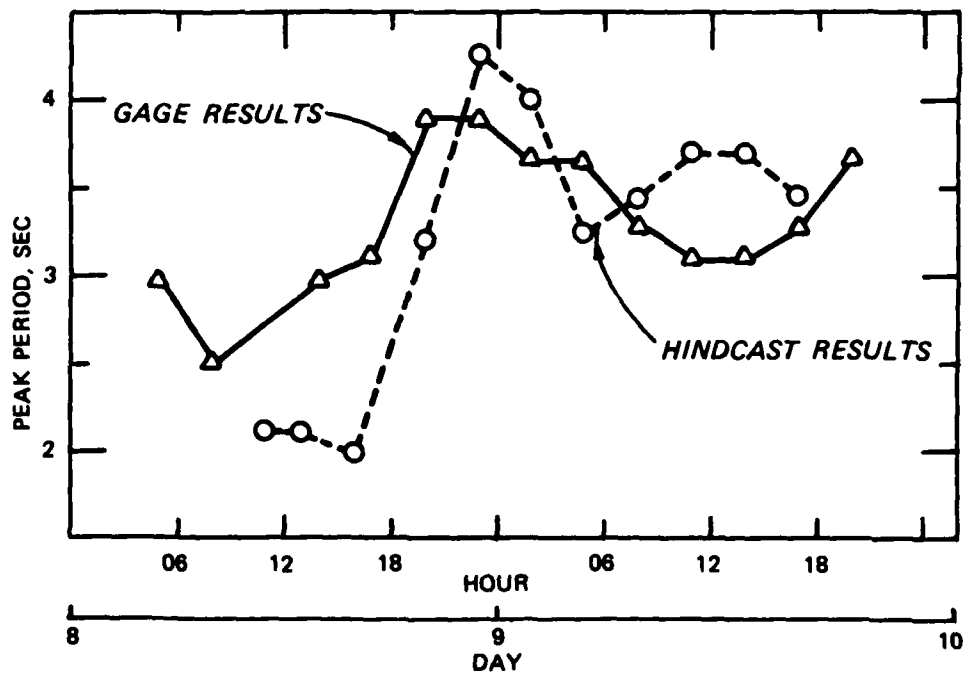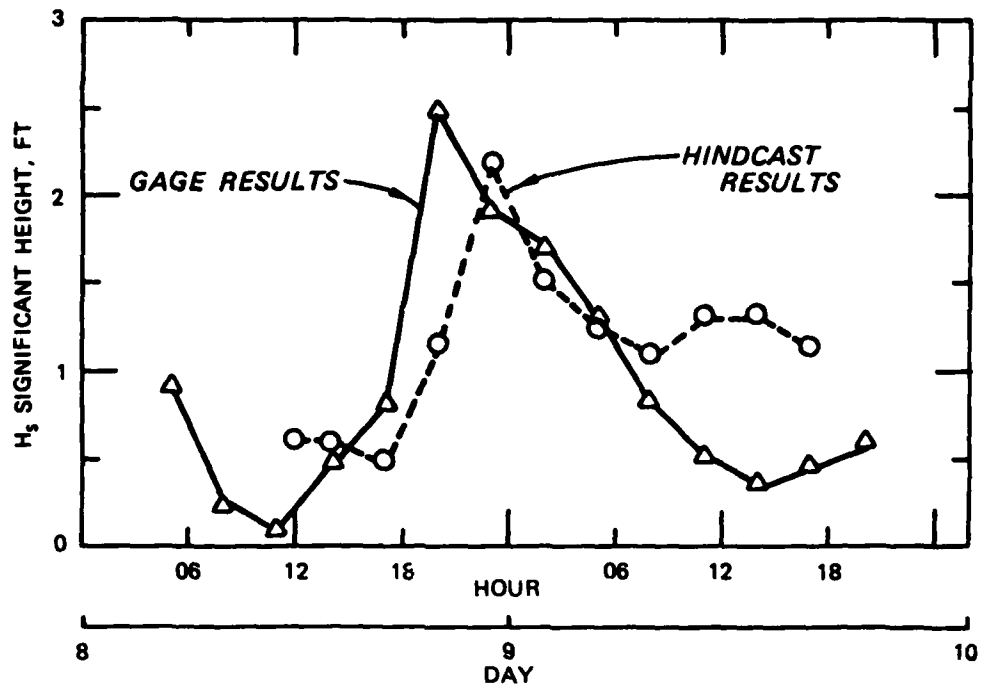wave-height data for Station 1 for BCT 1

A11

Figure A9. Comparison between measured and hindcast peak wave
period data for Station 1 for BCT 1
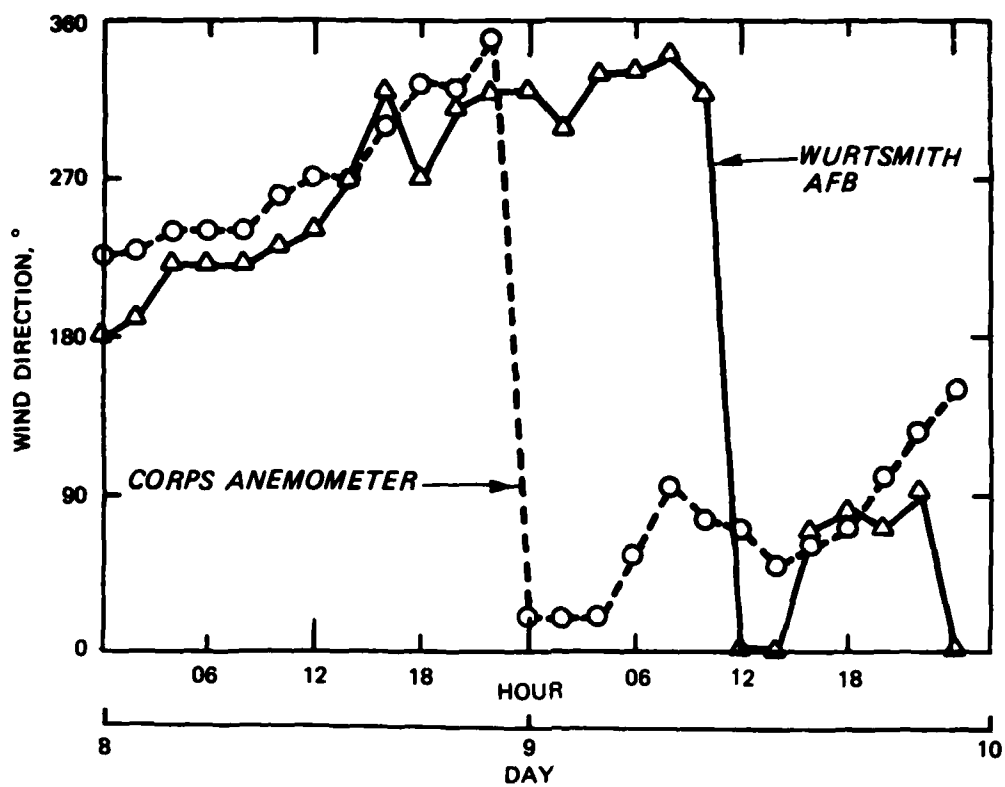
Figure A10.   Wind information data for BCT 2

Figure A11. Comparison between measured and hindcast significant
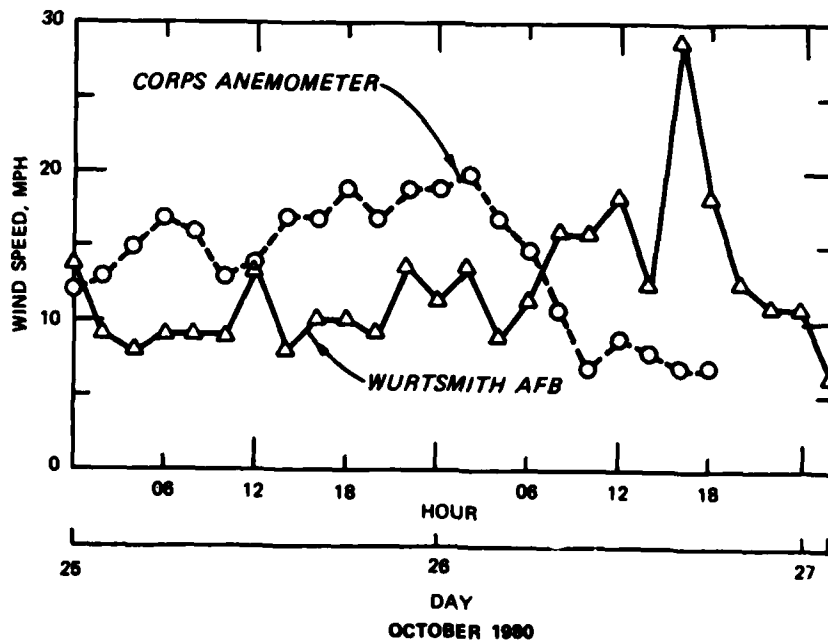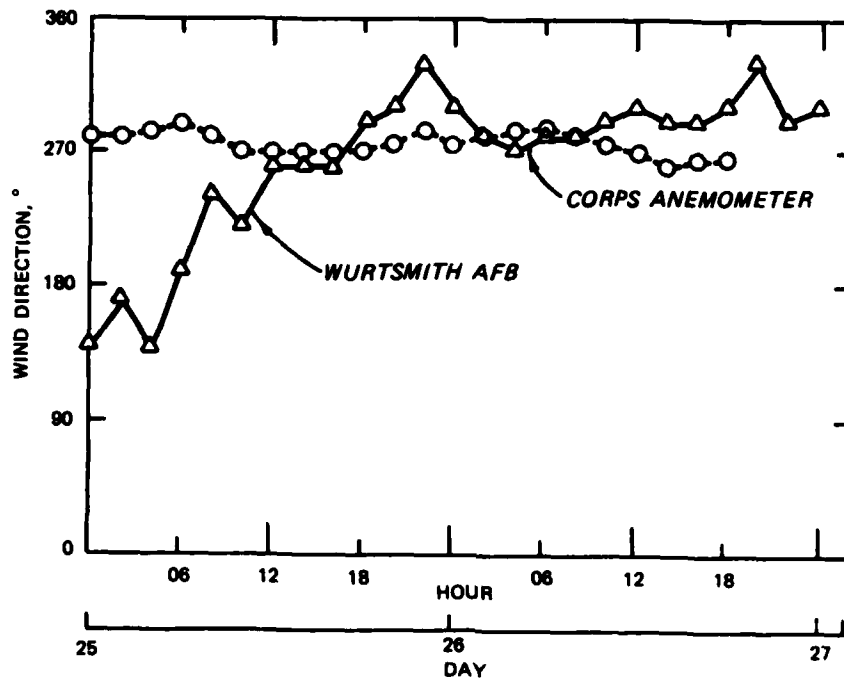wave height and peak period results for Station 1, BCT 2
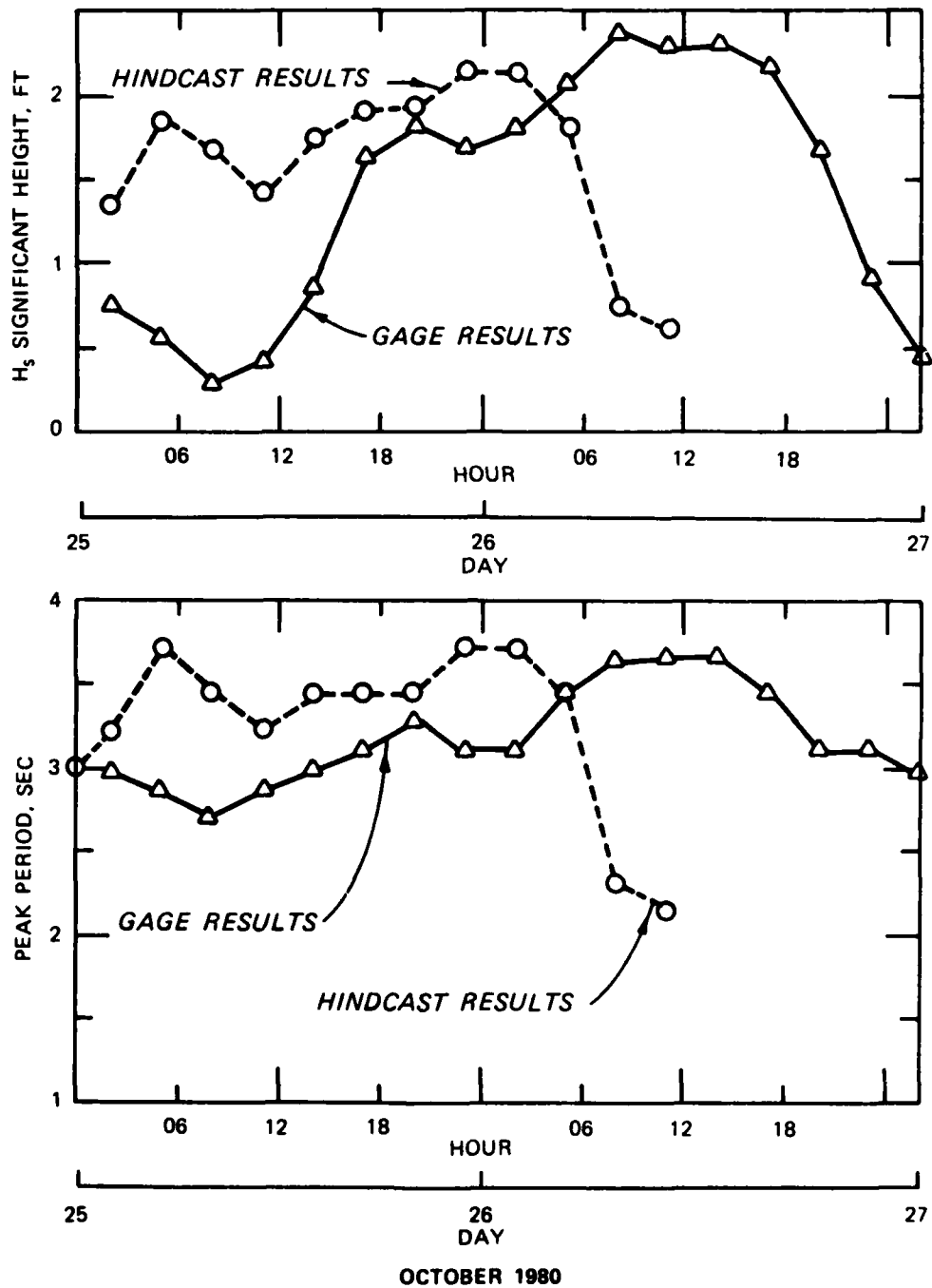
A14

Figure A12. Wind information data for BCT 3

Figure A13. Comparisons between measured and hindcast significant
wave height and peak period results for Station 1, BCT 3

A16

APPENDIX B: NOTATION

E	Final total energy at F_i
$E(f)$	Continuum energy density
$E(fj)$	Discrete energy density
E_o	Total energy resulting from a wind speed
E_{res}	Residual energy
E_1	Original total energy at F_{i-1}
E^*	Resultant discrete energy density spectrum at a given station
ff	Fraction factor
f_c	Lower frequency bounding the total energy
f_j	Discrete frequency band
$\tilde{f}_m$	Nondimensional peak frequency
F	Fetch length
F_t	Total fetch length
$F(x_j)$	The cumulative probability of occurrence of durations less than or greater than x for a particular H_j category
$F'(x_j)$	The cumulative probability that a duration event in category H_j will exceed or be less than length x
g	Acceleration due to gravity
$\bar{h}$	Mean water depth along F
h_i	Water depth at F_i
h_s	Water depth at a given station
H_j	Wave height
H_m	Maximum wave condition
H_s	Significant wave height
i	Increment counter
subscript j	Incremented wave-height counter
k_i	Wave number
K	Nonvarying parameter (and constants)
K_s	Shoaling coefficient
L_i	Wavelength
mx	Maximum duration

B1

n_j	Number of times waves exceed or become less than a particular wave height
$p(x_j)$	The probability of occurrence of a particular duration of wave heights greater than or less than H_j
Q	Dependent parameter
t	Total elapsed time since wind began to blow
t_{min}	Minimum duration condition
T	Peak wave period
T_s	Significant wave period
U	Wind speed
$\bar{x}$	Mean duration
x_{ij}	Duration of a single event with wave heights above or below level H_j
x_{jmax}	The maximum duration of waves above or below H_j
x_{jmin}	The minimum duration of waves greater than or less than H_j
$\tilde{X}$	Nondimensional fetch length
α	Phillips' equilibrium constant
γ	Weighting function
ΔF_i	Distance of wave travel within discrete fetch length
ζ_i	Independent parameter
θ_w	Wind direction
$\Phi(\omega_h)$	Nondimensional function
ϕf	Friction function
ψ	Direction of wave propagation

In accordance with letter from DAEN-RDC, DAEN-ASI dated
22 July 1977, Subject: Facsimile Catalog Cards for
Laboratory Technical Publications, a facsimile catalog
card in Library of Congress MARC format is reproduced
below.

Jensen, Robert E.
  Mississippi Sound wave-hindcast study main text and
appendices A and B / by Robert E. Jensen (Hydraulics
Laboratory, U.S. Army Engineer Waterways Experiment
Station). -- Vicksburg, Miss. : The Station ; Springfield,
Va. : available from NTIS, 1983.
  878 p. in various pagings : ill. ; 27 cm. --
(Technical report ; HL-83-8)
  Cover title.
  "April 1983."
  Final report.
  "Prepared for U.S. Army Engineer District, Mobile."
  A limited number of copies of Appendices C-G were
published under separate cover. Copies of this report and
Appendices C-G are available from National Technical
Information Service, 5285 Port Royal Road, Springfield,
Va. 22151.
  Bibliography: p. 54-56.

  1. Mathematical models. 2. Mississippi Sound.
3. Numerical analysis. 4. Water waves. I. United

Jensen, Robert E.
  Mississippi Sound wave-hindcast study main : ... 1983.
                                              (Card 2)

States. Army. Corps of Engineers. Mobile District.
II. U.S. Army Engineer Waterways Experiment Station.
Hydraulics Laboratory. III. Title IV. Series:
Technical report (U.S. Army Engineer Waterways Experiment
Station) ; HL-83-8.
TA7.W34 no.HL-83-8

ATE
ME